


Cite this: *RSC Adv.*, 2025, **15**, 2470

Received 26th November 2024  
Accepted 9th January 2025

DOI: 10.1039/d4ra08370a

[rsc.li/rsc-advances](http://rsc.li/rsc-advances)

## Progress in research on organic photovoltaic acceptor materials

Shijie Yuan, Wenzhen Luo, Mingfa Xie and Hongjian Peng \*

In the past two decades, organic solar cells (OSCs) have begun to attract attention as the efficiency of inorganic solar cells gradually approaches the theoretical limit. In the early development stage of OSCs, p-type conjugated polymers and n-type fullerene derivatives were the most commonly used electron donors and acceptors. However, with further research, the shortcomings of fullerene materials have become increasingly apparent. In recent years, non-fullerene acceptor materials, including small molecules and polymers, have emerged as promising alternatives to fullerene derivatives. This review summarizes various types of acceptor materials in OSCs and analyzes the advantages and disadvantages of each.

### 1 Introduction

Globally, energy and environmental issues have become a major challenge for mankind in the 21st century. Developing green, renewable and clean energy sources such as hydropower, solar energy, wind energy, tidal energy and bioenergy to replace fossil fuels is an effective way to achieve sustainable development and address the increasingly serious environmental problems.<sup>1</sup> Among them, solar energy, as one of the new clean energy sources, has attracted much attention because of its abundance, high energy yield, pollution-free production, renewability and other characteristics. Since 1954, G. L. Pearson *et al.*<sup>2</sup> at the American Bell Laboratory reported on monocrystalline silicon solar cells with a photoelectric conversion efficiency of about 6%. Since then, humanity has entered a new era of solar energy utilization.

Traditional solar cells, such as silicon-based and composite solar cells, have disadvantages such as complex preparation processes, significant pollution, and low efficiency.<sup>3</sup> Therefore, researchers have developed a new generation of solar cells, such as organic semiconductor solar cells and organic/inorganic hybrid solar cells. Among these, organic semiconductor solar cells have attracted widespread attention due to their simple material preparation, wide availability of materials, and the ability to achieve wet processing methods (such as the roll-to-roll method, and spin coating method).

The organic semiconductor solar cell is a type of solar cell that uses organic compound molecules with a large conjugate system, instead of conventional inorganic semiconductor, and employs organic compounds to undergo electron level transitions under light. Compared with traditional inorganic

semiconductor materials, it is difficult to form a periodic lattice structure. Furthermore, the intermolecular interactions are mainly dominated by van der Waals forces and  $\pi$ - $\pi$  stacking, making it difficult to form a continuous energy band. Organic semiconductor solar cells are similar to traditional solar cells in that their donor and acceptor components resemble the p-n heterojunction in inorganic solar cells, with the electron donor being p-type and the electron acceptor being n-type. When light interacts with donor molecules, the excited electron donor absorbs photons, causing an electron from its HOMO to transition to the LUMO, thereby forming an exciton. Typically, due to the lower ionization potential of the donor's LUMO than that of the acceptor's LUMO, electrons are transferred from the donor to the acceptor, completing the electron transfer and achieving exciton separation, as shown in Fig. 1.

There are many types of acceptors for organic solar cells, such as fullerene, non-fullerene, and polymers. In 1958, based on studies of photochemical processes in living organisms, Kearns and Calvin<sup>4</sup> first proposed the use of magnesium phthalocyanine (MgPc) and tetramethyl *p*-phenylenediamine (TM $\varphi$ D) oxidized by air as active substances to build a solar cell. The maximum voltage of the device is 200 mV. However, the

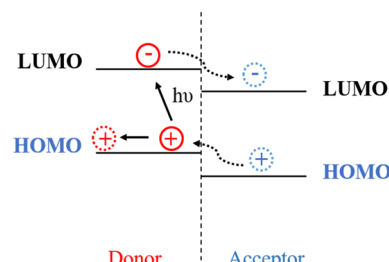


Fig. 1 Working principle of organic solar cells.



traditional Schottky battery construction method is essentially adopted, and the energy conversion efficiency is low. By 1986, on the basis of previous studies, Tang<sup>5</sup> used CuPc and imide (PV) as the active layer material to build a double-layer heterojunction battery. Its open circuit voltage ( $V_{oc}$ ) was about 450 mV, and the energy conversion efficiency (PCE) was nearly 1%. Owing to these research studies, organic solar cells then entered a new stage. In 1992, Sariciftci *et al.*<sup>6</sup> first applied  $C_{60}$  to organic solar cells, paving the way for the application of fullerenes and their derivative acceptors in organic solar cells. The first polymer acceptor cyanogen-modified polyethylene (CN-PPV) was produced in 1995 by Yu and Heeger.<sup>7</sup> However, small molecule non-fullerene acceptors appeared later at the beginning of the 21st century. The first reported small molecule non-fullerene acceptor was a thick polycyclic aromatic diimide acceptor. Among these, amides (PDIs) are the most widely studied. In recent years, organic solar cells have experienced rapid development. Owing to the development of small-molecule non-fullerene acceptor materials, the PCE of single-layer organic solar cells has exceeded 18%.<sup>8</sup> Its PCE is already comparable to that of early silicon-based solar cells, reaching

the commercial threshold. There are mainly two types of organic solar cells that are prepared based on the electron donor/acceptor system. One is a double-layer or multi-layer heterojunction organic solar cell, in which the electron donor and electron acceptor are sequentially stacked in the form of layered thin films to form a photoelectric conversion active layer. Another approach is to blend donor and acceptor materials to form a photovoltaic active layer, known as bulk heterojunction organic solar cells (BHJ-OSC) (Fig. 2).

Nowadays, increasingly more scientists are conducting research on OCS acceptor materials. Taking ScienceDirect as an example, by 2024, publications on "organic solar cell acceptor materials" increased by nearly threefold compared to 10 years ago (Fig. 3). This article introduces the development of OSCs and focuses on the research progress of high-performance acceptor materials for OSCs, including fullerenes and their derivatives, and non-fullerene acceptor materials (Table 1). In addition, we discuss the typical applications of high-performance acceptor materials in OSCs. Finally, we summarize the prospects and challenges of high-performance OSCs acceptor materials.

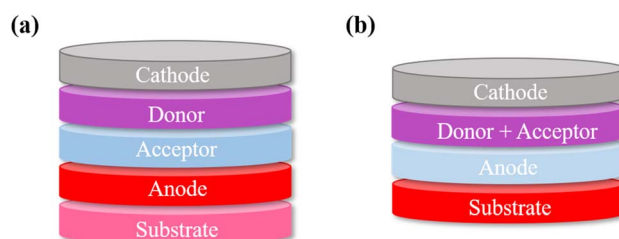


Fig. 2 Structure of OSCs: (a) double-layer heterojunction cell; (b) bulk-heterojunction cell.

## 2 Fullerenes and their derivatives

In 1995, Lepeq *et al.*<sup>9</sup> used Hummelen-optimized PC61BM<sup>10</sup> as the acceptor material and mixed it with MEH-PPV to prepare organic photovoltaic devices. Since then, fullerene derivatives have been the most important organic photovoltaic acceptor materials. Fullerene and its derivative acceptor materials are the first kind of acceptor materials used in organic solar cell devices. Because of their conjugated spherical structure, they have good electron transmission properties. However, they also have disadvantages, such as a narrow absorption band and ease

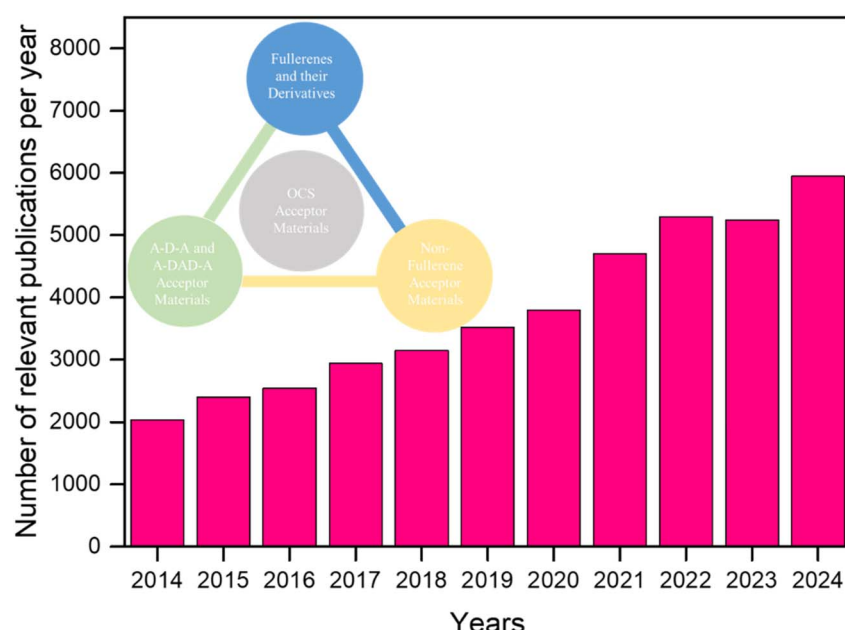


Fig. 3 Changes in the number of relevant literature publications over the years.



Table 1 Solar cell parameters of important acceptor materials

Acceptor	Donor	$J_{SC}$ (mA cm $^{-2}$ )	$V_{OC}$ (V)	FF (%)	PCE (%)
[70]PCBM <sup>12</sup>	MDMO-PPV	7.6	0.77	51	3
PCBM <sup>29</sup>	P3HT	11.3	0.65	57	4.2
FP <sup>30</sup>	P3HT	7.85	0.66	66.2	3.44
SIMEF <sup>32</sup>	BP	10.5	0.75	65	5.2
ICBA <sup>33</sup>	P3HT	9.67	0.84	67	5.44
NC60BA <sup>34</sup>	P3HT	9.88	0.82	67	5.37
P(PDI-BDT-O) <sup>42</sup>	PTB7-Th	11.51	0.8	51.1	4.71
PZ1 (ref. 45)	PBDT-T	16.05	0.83	68.99	9.19
PF3-DTC <sup>49</sup>	DTCO	15.75	0.943	68.2	10.13
PJ1 (ref. 51)	PBDT-T	20.7	0.9	70	14.4
FG6 (ref. 53)	PBDT-T	24.48	0.88	70	15.08
<i>d</i> BTIC $\gamma$ -EH <sup>54</sup>	PM6	21.43	0.92	73.28	14.48
2BTP-2F-T <sup>55</sup>	PM6	25.5	0.911	78.28	18.19
IE-4Cl <sup>58</sup>	PBDT-T	21.49	0.86	60	11.1
Phenyl-PDI <sup>74</sup>	PBT13T	6.56	1.024	54.59	3.67
INIC3 (ref. 96)	FTAZ	19.44	0.857	67.4	11.5
IC-C6IDT-IC <sup>99</sup>	PBDT-T1	14.21	0.9	61	7.8
L8-BO <sup>101</sup>	PM1	27.15	0.881	80.14	18.7
N3 (ref. 106)	PM6	26.2	0.862	72.7	16.42
BTP-4F-P3EH <sup>115</sup>	PBDT-T-2F	25.85	0.88	80.08	17.57

of aggregation within the visible light range.<sup>11</sup> To overcome these shortcomings, researchers have focused on the development of fullerene derivative acceptors represented by PCBM on the basis of C<sub>60</sub>, C<sub>70</sub> and other fullerene molecules.

## 2.1 The PCBM class of acceptors

PCBM materials are derived from fullerenes, so variations of the fullerene parent body can lead to different properties within the PCBM materials. The most common acceptor materials are PC<sub>61</sub>BM and PC<sub>71</sub>BM for both materials.

PC<sub>61</sub>BM quickly gained much attention after being synthesized and successfully applied in organic photovoltaic devices. The Wienk group<sup>12</sup> then tried to use C<sub>70</sub> to replace C<sub>60</sub> as the parent for the synthesis of PC<sub>71</sub>BM. Furthermore, organic photovoltaic devices were prepared with the polystyrene derivative MDMO-PPV as an electronic delivery system. Compared to PC<sub>61</sub>BM, studies have shown that the absorption peak of PC<sub>71</sub>BM is obviously redshifted in the UV-visible region, and the absorption range is wider, thus improving the photovoltaic performance. For photovoltaic devices with PC<sub>71</sub>BM as an acceptor and MDMO-PPV as a donor, the  $J_{SC}$  value is more than 50% higher than that of those with PC<sub>61</sub>BM as an acceptor under the same conditions. Meanwhile, the  $V_{OC}$  and PCE of the two devices are comparable. As a result, increasing the number of carbon atoms of the parent fullerene may improve the photovoltaic performance of the PCBM acceptor. In another study, Hummelen *et al.*<sup>13</sup> further used C<sub>84</sub> as the parent molecule to prepare the PC<sub>85</sub>BM material. However, the performance decreased significantly for the organic photovoltaic devices that used PC<sub>85</sub>BM as an acceptor material. Hummelen believed that the decrease of the HOMO-LUMO energy level difference of PC<sub>85</sub>BM may have led to the decrease of  $V_{OC}$ , and the large difference of the carrier mobility to the acceptor material may have resulted in the inability to achieve effective separation of

the photo excitons, thus reducing the overall performance of the device.

In addition to changing the parent molecule, using different modified structures is another common design strategy for optimizing PCBM. Research on modified structures mainly focuses on three aspects, namely the aromatic ring species, carbon chain length, and substituted ester groups.<sup>14</sup> Hummelen *et al.*<sup>15</sup> introduced methoxy, methyl sulfur, or fluorine atoms to the benzene ring of PC<sub>61</sub>BM. It was found that the introduction of different substituents can change the LUMO level of the PCBM material. The introduction of a methoxy group to the electron group can improve the LUMO level of the PCBM material, so as to get a higher  $V_{OC}$ . Yong and colleagues<sup>16</sup> substituted the structure of triarylamine and 9,9-dimethyl fluorene for the benzene ring to synthesize TPA-PC<sub>61</sub>BM and MF-PC<sub>61</sub>BM. Benefiting from the triarylamine and 9,9-dimethyl fluorene having stronger electron-donating properties than the benzene ring, they were able to increase the LUMO level of the molecules and  $V_{OC}$ . However, the larger volume of trianiline and 9,9-dimethylfluorene will reduce the electron mobility of the material. Furthermore, their effects cancel each other, such that there is little difference in the PCE between photovoltaic devices using TPA-PC<sub>61</sub>BM and MF-PC<sub>61</sub>BM as acceptors and those using PC<sub>61</sub>BM as acceptors. Most importantly, it is precisely because of the increase of the molecular volume and the destruction of symmetry that the crystallization property of the material is greatly reduced. Thus, the crystallization phenomenon of the active layer of the organic photovoltaic device is inhibited when the temperature increases, avoiding the destructive phase separation of the donor/acceptor and improving the thermal stability of the organic photovoltaic device. In addition to the above studies, the benzene ring can be replaced with thiophene,<sup>17,18</sup> selenophene,<sup>18</sup> pyrene<sup>19</sup> and others. The molecular structures of some PCBM acceptors are shown in Fig. 4.



Yongfang Li's group<sup>20</sup> studied the effect of the side alkyl chain length on the performance of PC<sub>61</sub>BM. Studies have shown that the length of the side alkyl chain has little effect on the HOMO and LUMO energy levels of PC<sub>61</sub>BM, but has significant effects on the absorption strength, electron mobility, morphology of the doped P3HT films and the interface structure of P3HT/PCBM, thus affecting the overall performance of photovoltaic devices. In this work, five acceptor molecules, F1–F5, were synthesized, and the side alkyl chain was successively

increased, as shown in Fig. 4. The PCE values of the devices with F1, F2 and F4 as acceptors were more than 3.5%. Conversely, the PCE values of the devices with F3 and F5 were lower than 3.0%. It can be seen from this result that the influence of the side alkyl chain length on the performance of PCBM is not linear. Therefore, the performance of PCBM cannot be analyzed simply from the length of the side alkyl chain.

In addition to changing the aromatic ring and side chain alkyl chain lengths, the properties of the molecule can be

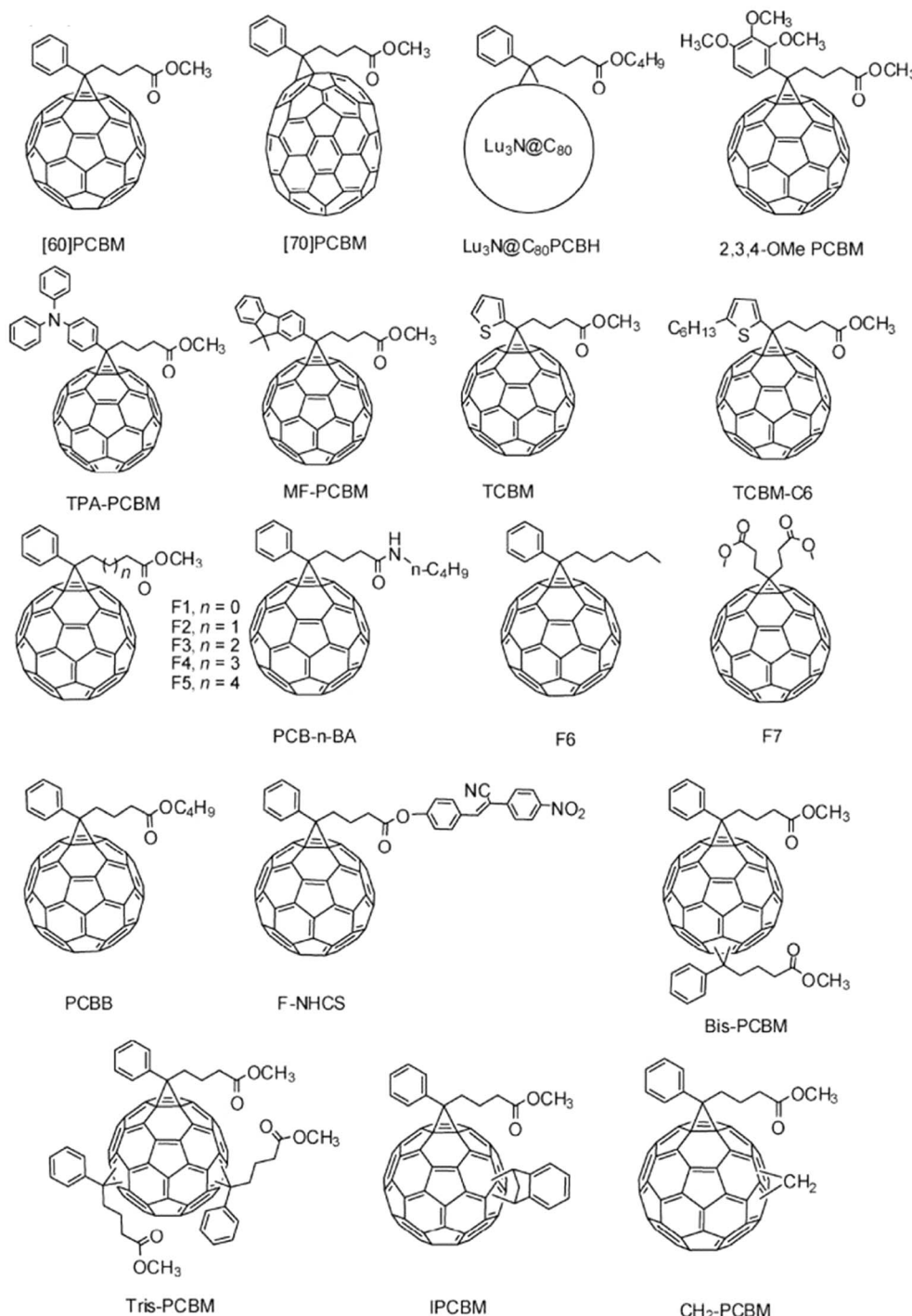


Fig. 4 Molecular structures of PCBM acceptors.



adjusted by replacing the ester group. Zheng *et al.*<sup>21</sup> replaced the ester methoxy in PCBM with a longer alkoxy carbon chain. They found that the electron mobility of the acceptor material gradually decreased with increasing alkoxy carbon chain length in the ester. Furthermore, the compatibility with the donor material MEH-PPV gradually improved, while the HOMO and LUMO energy levels remained almost unchanged. The overall performance of the photovoltaic devices increased first and then decreased. Thus, an appropriate growth of the alkoxy carbon chain is a reasonable means to improve the photovoltaic performance of the acceptor materials. Li and his colleagues<sup>22</sup> replaced the methyl ester group in PCBM with the *N*-butyl amide group, and synthesized PCB-*n*-BA, PCB-*t*-BA and MPCB-*t*-BA. Due to the presence of amino groups, hydrogen bonds of certain strength can be formed between molecules, thereby promoting the ordered arrangement of acceptor molecules. The effective intermolecular energy and electron transfer between the donor and the acceptor unit can be realized, which improves the photovoltaic performance of the device to a certain extent. The PCE of P3HT:PCB-*n*-BA reached 0.78%, higher than that of P3HT:PCBM by 0.59%. Mikroyannidis *et al.*<sup>23</sup> synthesized PCBC-NHCs containing a styrene vinyl phenol ester structure, which not only improved the solubility of the acceptor material in organic solvents, but also made the material have stronger absorption than PCBM in the range of 250–900 nm, showing better photovoltaic performance. In a recent study, Andrea *et al.*<sup>24</sup> introduced selenophenol, thiophene, and furan at the methyl ester group of PCBM, and compared their performance differences. The experimental results showed that compared with thiophene and furan, selenophenol substitution has higher stability. Thus, it can better reduce interface recombination in solar cells, optimize electron mobility, and charge extraction process.

Besides several research directions, embedded fullerene derivative acceptors were developed.<sup>25</sup> On the basis of PCBM to obtain two-addition, three-addition molding PCBM acceptor molecules is also an effective means to design new acceptor materials.<sup>26–28</sup>

## 2.2 Non-PCBM class of fullerene derivative acceptors

A non-PCBM fullerene derivative acceptor material was first obtained by Backer *et al.*<sup>29</sup> through the reaction of C<sub>60</sub> with 3,4-dibromomethyl benzoate, and modified to obtain the acceptor G1 of the dihydronaphthalene derivative. Although the photovoltaic performance of the acceptor was not significantly improved, the solubility of the acceptor material was greatly improved, providing a new approach for the modification of fullerene acceptor materials. The biggest difference between non-PCBM fullerene derivative acceptor materials and PCBM is whether the ternary ring can be obtained after the reaction of fullerene and modified molecules. In non-PCBM-like fullerene derivative acceptor materials, side chains are generally connected to the main body by means of five-membered rings, six-membered rings or open chains.

Matsumoto *et al.*<sup>30</sup> prepared a series of fullerpyrrolidine acceptor materials (FP). It has been found that halogen atoms in

the *o*-substituted compounds have better photovoltaic performance than the corresponding intermediate or *para*-substituted compounds. Compared with PC<sub>61</sub>BM, the PCE of fluorosubstituted fullerpyrrolidine is slightly increased, but the strong electron-taking group trifluoromethyl substitution will lead to a significant reduction of PCE. In contrast, the methoxy-substituted fullerpyrrolidine acceptor obtained a high  $J_{SC}$  (7.85 mA cm<sup>-2</sup>) and an optimal PCE value (3.44%).

In 2008, Matsuo *et al.*<sup>31</sup> synthesized fullersilane derivatives for the first time, and used SIMEF as the acceptor and porphyrin as the donor to construct p-i-n type photovoltaic devices.<sup>32</sup> The results show that SIMEF has suitable crystallization properties, and can form staggered cylindrical structures with porphyrins at the interface. Moreover, the size of the crystal column is suitable for charge separation and carrier transport, so better device performance can be obtained ( $V_{OC} = 0.75$  V,  $J_{SC} = 10.5$  mA cm<sup>-2</sup>, PCE = 5.2%).

As with PCBM-like acceptors, the multiple addition of fullerenes is also an effective way to design new acceptor materials for non-PCBM-like fullerenes derivatives. Li *et al.*<sup>33</sup> reported on a kind of inden-C<sub>60</sub> double adduct (IC<sub>60</sub>BA, structure shown in Fig. 5). Compared with PCBM, the LUMO energy level of this new acceptor was significantly higher than that of PCBM, so it could effectively increase the  $V_{OC}$  of photovoltaic devices. The  $V_{OC}$  of the IC<sub>60</sub>BA device reached 0.84 V, an increase of 0.26 V. At the same time, IC<sub>60</sub>BA also has greater absorption intensity in the visible region. In terms of visible light absorption, IC<sub>60</sub>BA has better photovoltaic performance than PCBM. The experimental determination of the P3HT:IC<sub>60</sub>BA device reached 5.44%. Chunru Wang *et al.*<sup>34</sup> synthesized a C<sub>60</sub> double adduct based on dihydronaphthalene (NC<sub>60</sub>BA, structure shown in Fig. 5). Compared with the PCBM material, NC<sub>60</sub>BA has a significantly improved LUMO energy level and stronger absorption in the visible region. Furthermore, due to the introduction of two dihydronaphthalene groups, the molecular crystallization property is reduced. Thus, the aggregation will not easily occur during heating, which improves the thermal stability of organic photovoltaic devices.

In addition to optimizing fullerene molecules as mentioned above, introducing metal ions into fullerenes is an important method for regulating their properties. Metal ions can increase the LUMO level of fullerenes, making them more conducive to electron reverse transfer.<sup>35</sup> Feng *et al.*<sup>36</sup> demonstrated through calculations that the addition of rare earth metals such as Er has higher and more tunable LUMO orbital energy characteristic values than fullerene itself, and results in considerable kinetic stability. These results provide favorable conditions for photovoltaic devices as innovative acceptor materials to match donor acceptor system energy levels. The favorable conditions for metal fullerene as an electron acceptor in organic solar cell devices have been demonstrated.

## 3 Non-fullerene acceptor materials

### 3.1 Polymer acceptor materials

Polymer acceptor materials are another very important organic photovoltaic acceptor materials. Compared with fullerene



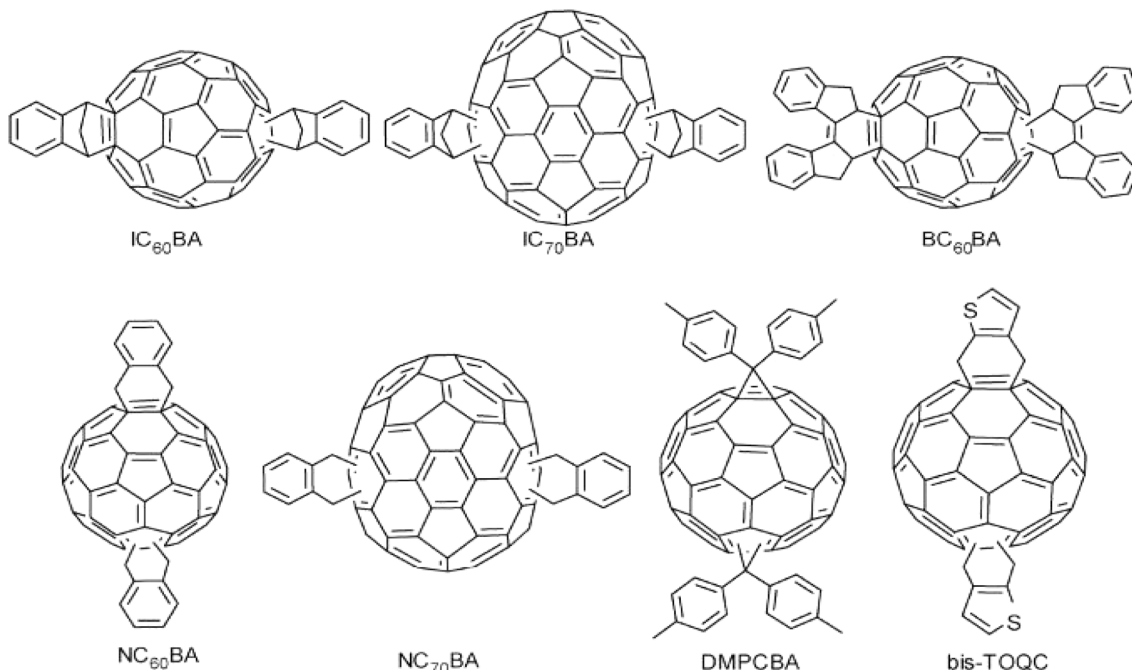


Fig. 5 Molecular structures of non-PCBM acceptors.

acceptor materials, polymer acceptors can more conveniently regulate HOMO and LUMO energy levels, so as to obtain acceptor materials with different properties. At the same time, the polymer has certain advantages in thermal properties and stability of the molecular morphology, which is convenient for the preparation of large-area devices. In recent years, the strategy of the narrow band gap small molecule acceptor (PSMA) proposed by Yongfang Li's research group at the Chinese Academy of Sciences has further advanced the polymerized small molecule acceptor (PSMA) materials to new limits.<sup>37</sup>

**3.1.1 The PPV derivative acceptor.** As mentioned earlier, the PPV derivative acceptor is the earliest used polymer acceptor. Yu and Heeger<sup>7</sup> first used MEH-PPV as a donor and CN-PPV as an acceptor to prepare all-polymer organic photovoltaic cells with PCE values of 0.25% under light irradiation at  $20 \text{ mW cm}^{-2}$ . Furthermore, Li *et al.*<sup>38</sup> synthesized DOCN-PPV by moving the modification position of the cyano group from the vinylidene unit to the benzene ring. The UV-visible absorption band edge was 625 nm, and the corresponding band gap was about 2.0 eV. With DOCN-PPV as an acceptor and PTZV-PT as the donor, the PCE of organic photovoltaic devices reached 0.8% (Fig. 6).<sup>39</sup>

**3.1.2 A D-A copolymer acceptor based on dense polycyclic aromatic diimides.** The D-A copolymer is a polymer organic

photovoltaic material formed by the co-polymerization of the donor unit and the acceptor unit. Because of the push-pull effect of electrons inside the molecules, the effective separation of light excitons can be promoted. At the same time, the energy level and photovoltaic performance of the polymer can be effectively regulated by changing the donor unit and the acceptor unit.<sup>40</sup>

Zhan *et al.*<sup>41</sup> synthesized a D-A copolymerized acceptor material PDI-DTT by using perylene diimide (PDI) derivatives and trithiophene as raw materials. The electron mobility of this material reached  $1.3 \times 10^{-2} \text{ cm}^2 (\text{V}^{-1} \text{ s}^{-1})$ , with a certain absorption throughout the visible light region and extending to the near-infrared region (about 850 nm), exhibiting better photovoltaic performance. With PDI-DTT as an acceptor and double (thiophene vinyl-substituted polythiophene) as the donor, the  $V_{OC}$  of photovoltaic devices is 0.63 V and the PCE is more than 1%. On this basis, the influence of the molar ratio of donor/acceptor units on the properties of acceptor materials was further studied. When the molar ratio of the donor/acceptor units is 2 : 1, the device performance is highest and the efficiency (PCE) is 1.48%.

Zhang and his colleagues<sup>42</sup> synthesized one-dimensional conjugated polymer acceptor P(PDI-BDT-O) and two-dimensional conjugated polymer acceptor P(PDI-BDT-T) using PDI derivatives and benzodithiophene as raw materials. The study showed that the two-dimensional structure of the N-type conjugated polymer was also superior to the corresponding one-dimensional polymer. The absorption spectrum of the P(PDI-BDT-T) film is redshifted by about 10 nm compared with P(PDI-BDT-O), which is due to the presence of conjugate side chains in the two-dimensional polymer P(PDI-BDT-T). The bandgap widths of P(PDI-BDT-O) and P(PDI-BDT-T) are 1.66 eV

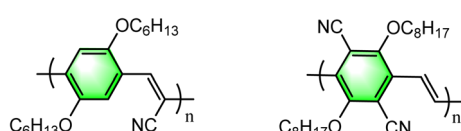


Fig. 6 Molecular structures of CN-PPV and DOCN-PPV.



and 1.64 eV, respectively. With P(PDI-BDT-T) as an acceptor and PTB7-Th as the donor, the PV devices can reach a maximum PCE of 4.71% and  $V_{OC}$  of 0.80 V (Fig. 7).

In 2008, Guo *et al.*<sup>43</sup> first synthesized a new polymer acceptor N2200 using naphthalimide (NDI). Since then, N2200 has been widely studied as a classic polymer acceptor material in the field of solar cells. In a recent study, researchers developed a high-performance non-fullerene ternary PSC by incorporating N2200 into a binary blend membrane composed of the wide bandgap conjugated polymer PTzBI-2FP and small molecule non-fullerene acceptor ITIC-4F. Attributed to the effective energy transfer, enhanced charge carrier mobility, and improved morphology, the three obtained components showed an excellent power conversion efficiency of 13.0%.<sup>44</sup>

**3.1.3 The PSMA acceptor.** Since 2015, the narrow band gap small molecule acceptor has replaced the traditional fullerene acceptors because of its characteristics of controllable electronic energy level and strong absorption of the visible light area. Based on these characteristics, researchers proposed the PSMA strategy in 2017, hoping to synthesize new acceptors with the advantages of both non-fullerene small molecule acceptor and polymer acceptors.<sup>45</sup>

In 2017, based on the small-molecule acceptor IDIC-C16, the PSMA acceptor PZ1 was synthesized by Li *et al.*<sup>45</sup> In order to facilitate polymerization, researchers prepared PZ1 through the copolymerization of idic-C16-Br and thiophenone. Compared with IDIC-C16, the absorption spectrum of PZ1 is redshifted by about 50 nm, and the absorption band edge is 800 nm. Meanwhile, the LUMO level of PZ1 is slightly higher than that of IDIC-C16. The all-polymer organic photovoltaic cell with PZ1 as the acceptor and PBDBT-T as the donor exhibits a  $V_{OC}$  of 0.83 V,  $J_{SC}$  of 16.05 mA cm<sup>-2</sup>, FF of 68.99%, and 9.19% PCE, which is significantly higher than the PCE of the corresponding IDIC-C16-based device (3.96%). It was also found that PZ1 has good solubility in organic solvents, and has good film-forming performance. Compared with IDIC-C16, PZ1 has improved thermal stability, showing the advantages of both polymer acceptor and non-fullerene small molecule acceptor. This research led to a new strategy for the design of polymer acceptors, receiving extensive attention.

Yao *et al.*<sup>46</sup> made improvements on the basis of PZ1 by replaced the thiophene unit with a structural unit based on benzodithiophene, and synthesized PFBDT-IDTIC, which can achieve 10.3% PCE at 0.97 V high  $V_{OC}$  by pairing with PM6. Ultraviolet-visible spectroscopy showed that the absorption band edge of the PFBDT-IDTIC thin film was about 767 nm, corresponding to a band gap of 1.62 eV. Compared with the absorption band edge of PZ1, there was a certain blue shift. At the same time, there was an obvious feature at 648 nm. These indicates that the PFBDT-IDTIC solid polymer molecular chains have strong aggregation and efficient stacking properties.

Li *et al.*<sup>47</sup> and Fan *et al.*<sup>48</sup> replaced the donor units copolymerized with IDIC with the derivatives of thiophene (BT), and synthesized the PIDIC2T series of acceptors and PF2-DT series of acceptors respectively. Li *et al.*<sup>47</sup> synthesized PIDIC2T2F and PIDIC2T2Cl by halogenation modification on the basis of the simple BT unit. They found that halogen substitution could enhance  $\pi$ - $\pi$  stacking between molecules, which was speculated to be due to C-X···H-C and C-X···S, which indicates the existence of two non-covalent interaction forces. Fan *et al.*<sup>48</sup> used IVA group elements (C, Si, Ge) to bridge two thiophene rings in the BT unit, and synthesized three polymer acceptant materials, PF2-DTC, PF2-DTSi and PF2-DTGe, respectively. Through research studies, it was found that the bridging atoms had little effect on the molecular energy level. However, it can significantly affect the absorption coefficient, crystallization capacity and electron mobility of the polymer acceptors. Fan *et al.*<sup>49</sup> also increased the number of thiophene rings in IDIC units on the basis of PF2-DTC, and synthesized two acceptor materials, PF3-DTC and PF3-DTCO. Compared with PF2-DTC-based devices, PF3-DTC-based devices show similar  $J_{SC}$  but significantly reduced FF. This may be due to the strong self-aggregation of PF3-DTC in the blend film, leading to excessive phase separation. Nevertheless, PF3-DTCO-based blend films show better  $\pi$ - $\pi$  packing distance and phase separation size. The performance of PF3-DTCO acceptor devices also reached a good level ( $V_{OC} = 0.943$  V,  $J_{SC} = 15.75$  mA cm<sup>-2</sup>, FF = 68.2%, PCE = 10.13%) (Fig. 8).

Fan *et al.*<sup>50</sup> also introduced non-conjugated units into the polymer acceptor skeleton in a pioneering study to synthesize

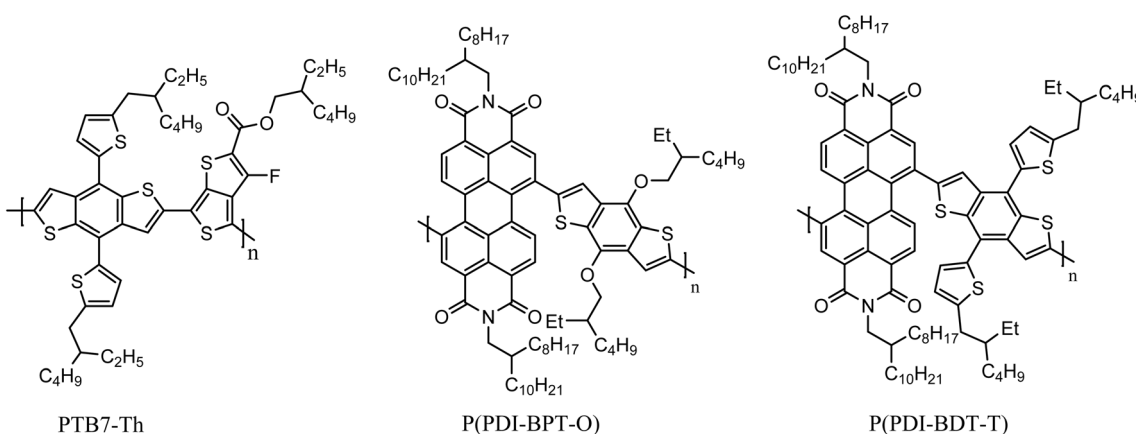


Fig. 7 Molecular structures of D–A copolymer acceptors based on polycyclic aromatic diimide.



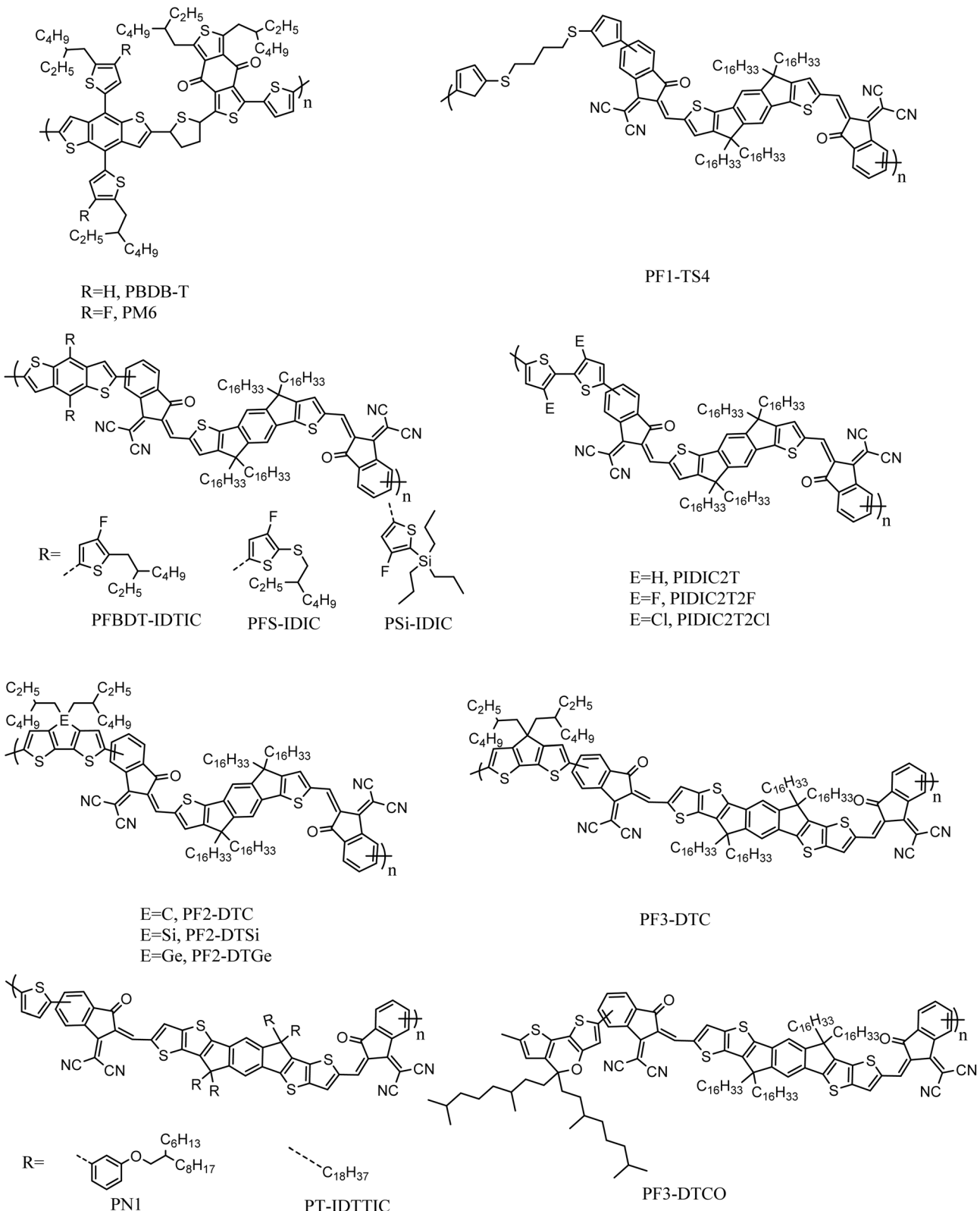


Fig. 8 Molecular structures of the PSMA series of acceptors.

PF1-TS4. It was found that PF1-TS4 exhibits physical properties similar to those of conjugated polymers, with an optical band gap of 1.58 eV and an absorption coefficient higher than

$10^5$  cm<sup>-1</sup>, as well as a high LUMO energy level and suitable crystallinity. After coordination with the polymer donor PM6, 8.63% PCE was achieved, which was a great improvement

compared with the small-molecule acceptor material IDIC-16C. In addition, PF1-TS4-based all-polymer solar cells have good thermal stability, with a PCE retention rate of 70% after 180 h at 85 °C. This provides a new approach for the design of polymer acceptor materials.

In recent years, with the emergence of the star molecule Y6, PSMA acceptor materials based on Y6 have received increased attention. Yong Cao *et al.*<sup>51</sup> synthesized a novel PSMA acceptor PJ1 by copolymerizing Y6 with thiophene, which has a narrow band gap of 1.4 eV and a high absorption coefficient of  $1.39 \times 10^5 \text{ cm}^{-1}$ . When PJ1 was blended with PbDBT-T, the PCE value of the device was 14.4%. This was mainly due to the wide absorption, efficient charge separation, and low energy loss of PJ1. With further research developments, many polymer solar cells composed of PSMA-based acceptor materials now currently have PCE values exceeding 18%. Bi *et al.*<sup>52</sup> systematically studied the effect of the molecular weight of polymer acceptors on the phase transition process, morphology, and photovoltaic properties by using the PYIT monomer (PYIT1), and low molecular weight PYIT and high molecular weight PYIT. The study showed that adjusting the molecular weight can effectively regulate the phase transition process of polymer acceptors and their interaction with polymer donors. When PBQx Cl is used as the donor and low molecular weight PYIT is used as the acceptor, binary All PSC with PCE = 18.39% can be achieved.

### 3.2 Oligo non-fullerene small molecule acceptor materials

Recently, Guijarro *et al.*<sup>53</sup> designed several materials having different terminal units, but the same cyclopentadienylthiophene vinylene (CPDTV) trimer as the electron-donating units (FG10 as IC, FG6 as IC-4Cl, FG8 as IC-4F). FG6 and FG8 exhibit redshifted absorption spectra and higher electron mobility. With the increased halogenation at the IC end, the dielectric constant of these materials will also increase, leading to a decrease in the exciton binding energy. This is beneficial for the dissociation of excitons and subsequent charge transfer. When using these acceptor materials to construct OSCs with PBDB-T, FG6 and FG8 exhibited high PCE values of 15.08% and 12.56%, respectively.

In May 2022, Feng *et al.*<sup>54</sup> synthesized a series of acceptors, including small molecule acceptors, oligomeric acceptors and polymer acceptors, known as BTIC-EH, dBTIC $\gamma$ -EH, dBTIC $\gamma$ -BO, tBTIC $\gamma$ -BO and pBTIC $\gamma$ -OD. It was found that the oligomer acceptor has almost the same thermal stability as the polymer acceptor, and that both oligomerization and polymerization can lower the energy level and thus provide a higher probability of exciton dissociation than the small molecule acceptor. When combined with PM6, these oligomer acceptor-based BHJ devices showed higher charge-carrier mobility and lower charge recombination compared to the BTIC-EH and pBTIC $\gamma$ -OD devices, indicating better charge transport capacity. Meanwhile, OSCs based on dBTIC $\gamma$ -EH:PA6, dBTIC $\beta$ -BO:PM6 and tBTIC $\gamma$ -Bo:PM16 showed better photovoltaic performance. Among these devices, dBTIC $\alpha$ -EH:PM16 obtained the best PCE of 14.48%. dBTIC $\gamma$ -EH also showed better photovoltaic

performance in Q-PHJ devices than BTIC-EH and pBTIC $\gamma$ -OD when combined with PBQx-H-TF, the polymer donor. The device based on dBTIC $\gamma$ -EH: PBQx-H-TF showed 16.06% PCE, which is the highest value of oligo-acceptor-based OSC reported in the literature.

Zhixiang Wei *et al.*<sup>55</sup> designed an N- $\Pi$ -N type oligomeric acceptor 2BTP-2F-T in June 2022. Using its corresponding monomers and polymers as references, the advantages of 2BTP2F-T were demonstrated, including higher absorption coefficients, improved electron mobility, less dependence on molecular filling, and easier morphological control using polymer donors. When PM6 was used as a donor, PM6/2BTP-2F-T exhibited superior advantages over their monomer and polymer blends: (1) more favorable morphology, including a minimal energy disorder  $\pi$ - $\pi$  stack and an appropriate interpenetrating network; (2) improved charge characteristics, including higher hole/electron mobility, longer charge lifetime and faster charge extraction; (3) more efficient generation with the same energy loss; (4) compared with similar polymer products, it has better photo dip stability and thermal stability. With an efficiency of more than 18% combined with increased stability, the 2BTP-2F-T OSCs are indicative of a bright future for N- $\Pi$ -N oligo acceptor OSCs.

### 3.3 Small-molecule acceptor material

The non-fullerene small molecule acceptor (NFSMAS) is one of the latest organic photovoltaic acceptor materials. It is characterized by a controllable energy level, convenient synthesis, easy processing and good solubility.<sup>56</sup> NFSMAS have better absorption properties in the visible region than fullerenes and their derivative acceptor materials, so they have received extensive attention.

**3.3.1 Non-heavy ring-like small molecule acceptors.** In addition to creating large fusion ring systems, another strategy for hardening the acceptor backbone is to use “conformational locking”, which utilizes non-covalent interactions such as intramolecular hydrogen bonding to lock the coplanar conformation. This strategy has previously been used to design polymers with high carrier mobility. Since adjacent aromatic rings are connected by single bonds, the synthesis of such conformation-locked NFA is easier than ring fusion.

**3.3.1.1 IEIC acceptor.** IECE is a non-fullerene electron acceptor based on indeno [1,2-*b*:5,6-*b'*] dithiophene (IDT) and 2-(3-oxo-2,3-dihydroindenyl-1-ethylidene) malondinitrile (INIC). In 2014, the Lin group<sup>57</sup> reported that IECE achieved improved electronic performance due to its terminal being blocked by electron-withdrawing INCN groups, unlike fullerene acceptors with poor electronic performance. Meanwhile, IEIC acceptors have high thermal stability and strong light absorption in the range of 500 to 700 nm. Most importantly, IEIC has energy levels that match some traditional narrow bandgap donor polymers, such as PTB7-TH. In PSC without fullerene based on both donors and acceptors, with perylene diimide derivatives as the cathode interlayers, a 6.3% PCE was observed. In another study, Hong<sup>58</sup> conducted research on the performance of IEIC and its halogen derivatives. Researchers combined these three



acceptors with PBDB-T and PBDB-TF donor polymers to form six sets of OSC devices, which were influenced by the similar chemical structure of the D/A combination, bringing similar charge transfer properties to these OSCs. Among the three acceptor materials mentioned above, chlorinated IEIC (IE-4Cl) achieved a suitable molecular energy arrangement by adjusting its bandgap structure, exhibiting 11.1% PCE and 0.64 eV of  $E_{loss}$ , which were all higher than that of IECE (Fig. 9).

**3.3.1.2 Tertiary thiophene [3,2-*b*] thiophene type acceptor.** The molecular stacking of organic semiconductors has a great influence on the exciton and charge properties of their solid films, which strongly influences the photovoltaic performance of the derived solar cells. The Y-series of acceptors have been ring-fused to form a three-dimensional (3D) stacking network in the crystal, constructing channels and interconnection nodes to enhance the exciton and charge transport. However, it has been reported that most NFREAs are stacked into 2D layered lattices and lack interlayer continuity, which may limit the carrier and exciton dynamics of NFREAs. Recent studies have shown that a class of non-fusion acceptors characterized by spatial obstruction of aromatic side chains, such as A4T-16 and 2BTh-2F,<sup>59,60</sup> exhibit 3D networks in crystals, achieving about 15% of the prominent PCE of NFREAs-based OSC.

On this basis, Changzhi Li *et al.*<sup>61</sup> selected symmetric and asymmetric diarylamine chloride as spatial aromatic chains on the main chain of the tertiary thiophene [3,2-*b*] thiophene. They successfully synthesized two high-performance non-thick ring electron acceptors (L1 and L2), and revealed that halogen substituents on aromatic chains promote the densely stacked 3D networks of molecules in solid form. The successful

synthesis resulted in an efficiency of 16.2% for the derived OSCs. It is by far the highest number of OSCs composed of NFREAs. It provides multiple intermolecular interactions *via* chlorinated aromatic chains on NFREAs to interlock cross-molecular arrays to construct tic-tac-toe type 3D stacking networks. Furthermore, in contrast to symmetrical L1 (which has four chlorine atoms), the asymmetric chlorination of L2 (methyl groups replacing half chlorine atoms) allows for fine regulation of molecular interactions and the photoelectric properties of the acceptor, while preserving the required 3D stacking, thus improving the optical voltage parameters for high-performance OSCs. Meanwhile, L2-based OSCs demonstrated excellent operational stability at one solar equivalent without UV filtration, revealing a T80 lifetime of 17 241 hours from linear extrapolation. This study demonstrates that new design principles for organic semiconductors have the potential to lead to efficient, stable and low-cost organic photovoltaics.

**3.3.2 Thick ring-like small molecule acceptors.** Electron acceptors are a key component of the active layer of organic solar cells. From the development of electron acceptor materials, thick ring acceptor materials mainly include aromatic diimide acceptors, fullerene acceptors, A-D-A type thick ring acceptors and A-DA'D-A type thick ring acceptors. Fullerene derivatives and thick aromatic diimide acceptors were widely used as electron acceptors in early studies on OSCs. However, both recipients had inevitable drawbacks, and the efficiency of the organic photovoltaic devices was greatly improved upon the proposed use of A-D-A and A-DA'D-A-type acceptors.

**3.3.3 Gelled polycyclic aromatic diimide acceptors.** Gelled polycyclic aromatic diimide, especially naphthalene diimide

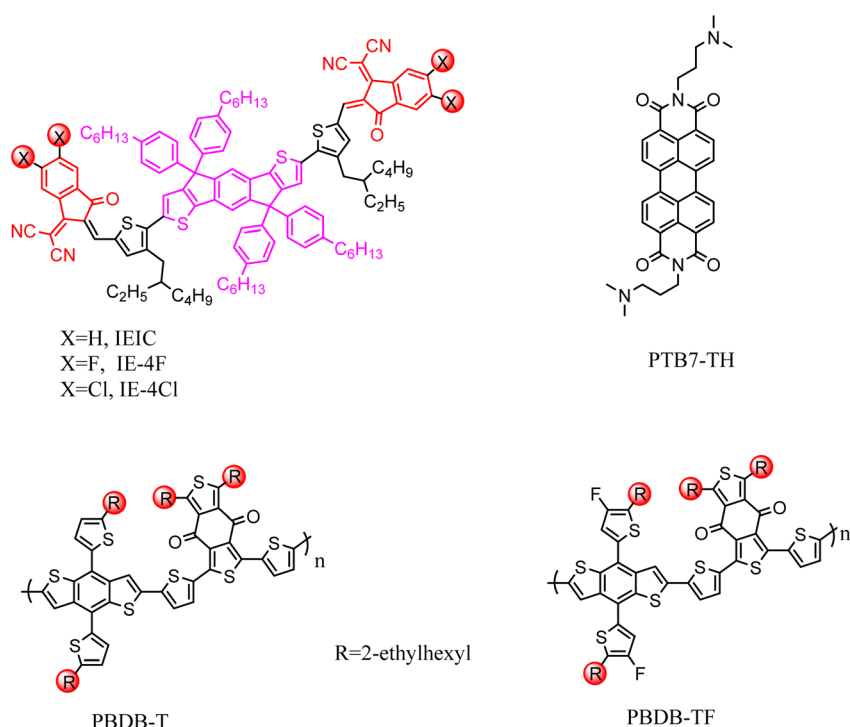


Fig. 9 Molecular structures of IEIC and some donor polymers.



(NDI) and perylene diimide (PDI), were first applied in various organic electronic devices due to their high electron affinity, electron mobility and good stability.<sup>62</sup> Albertus *et al.*<sup>63</sup> also self-assembled perylene diimide derivatives with the small donor molecule oligophene (OPV) into nanofibers through hydrogen bonding, so as to study the photoelectric properties of perylene diimide. This was the first attempt to use a gelled polycyclic aromatic diimide as an organic photovoltaic acceptor material.

Although dense polycyclic aromatic diimide acceptor molecules have the abovementioned advantages, the rigid plane structure of the aromatic system determines the strong  $\pi$ – $\pi$  stacking between the acceptor molecules. This leads to the excessive phase separation of the mixed film with thick polycyclic aromatic diimide, which reduces the charge transport performance. There are two solutions: one is to introduce large barrier groups into the molecule to distort the molecule and destroy the plane structure; the other is to connect multiple acceptor molecules through a central unit or single bond to construct a non-planar structure.

**3.3.4 Small molecule acceptor materials based on NDI.** In 2011, Jenekhe *et al.*<sup>64</sup> synthesized the NDI-nTH and NDI-nT series of novel acceptor molecules by introducing oligothiophene units with different degrees of polymerization into two opposite  $\beta$  sites of the naphthalene ring. The results show that both NDI-nTH and NDI-nT materials have high electron mobility, and the NDI-4TH film has the highest electron mobility ( $9.0 \times 10^{-4} \text{ cm}^2 (\text{V}^{-1} \text{ s}^{-1})$ ), while the NDI-2TH film has the lowest electron mobility ( $5.0 \times 10^{-6} \text{ cm}^2 (\text{V}^{-1} \text{ s}^{-1})$ ). However, the solar cells prepared by blending with P3HT have a higher  $V_{\text{OC}}$  (up to 830 mV), but a lower  $J_{\text{SC}}$  (up to 3.43 mA  $\text{cm}^{-2}$ ), and a maximum PCE of 1.5% (P3HT:NDI-3TH), which was the highest efficiency ever achieved by a small-molecule acceptor based BHJ cell at the time.

Roshan and his colleagues<sup>65</sup> studied the effects of nitrogen atoms of NDI and substituents on naphthalene rings on the photovoltaic performance. By introducing different linking groups between thiophene and NDI imide nitrogen atoms, six small molecule acceptor molecules RF1–RF6 were synthesized. The substituent group on the naphthalene ring in RF1, RF3 and RF5 was cyclohexyl amino, while the substituent group on the naphthalene ring in RF2, RF4 and RF6 was 2-ethylhexyl amino. Roshan believed that the changes of these substituents had little influence on the optical and electrochemical properties of the acceptor molecules, and had significant influence on the morphology of the blend film and device properties. The results show that the six RF1–RF6 molecules have similar absorption spectra and CV curves, but exhibited very different photovoltaic properties. The best device performance is achieved by using a methylene group as the connecting group and a naphthalene ring substituent group as the cyclohexyl amino. The second is the molecule (RF5) with phenyl as the linking group and naphthalene as the cyclohexyl amino group. Through AFM characterization, it was found that different substituents strongly influenced the phase separation size. The phase separation between ethyl and phenyl as linking groups (RF4–RF6) and P3HT was smaller than that between methyl and methyl as linking groups (RF1 and RF2). Therefore, it could be inferred

that the miscibility of P3HT and methyl as linking groups was poor.

In addition to modification on the basis of the NDI monomer, the use of a small molecular unit to connect two NDI molecules is another strategy for designing acceptor materials. This approach can destroy the overall planarity of the molecule, and thus reduce excessive aggregation between acceptor molecules. In 2014, Zhan *et al.*<sup>66</sup> synthesized two kinds of nonfullerene small molecule acceptor materials with a NDI dimer structure, Bis-NDI-T-EG and Bis-NDI-BDT-EG, using thiophene (T) and benzodithiophene (BDT) as the linking units. The DFT calculation showed that both acceptor molecules showed a distorted main chain conformation, which is beneficial to reducing the aggregation capacity. Furthermore, they showed weak absorption in the visible region, which is an improvement over the acceptor materials based on the NDI monomer. For PBDTTT-C-T:Bis-NDI-T-EG and PBDTTT-C-T, the PCE of the Bis-NDI-BDT-EG photovoltaic devices is 1.31% and 1.24%, respectively. Later, nonfullerene small molecule acceptor materials with a NDI dimer structure such as dibenzoxiloxane<sup>67</sup> and vinylidene<sup>68</sup> were synthesized.

**3.3.5 Small molecule acceptor materials based on PDI.** PDI has received widespread attention due to its excellent electron acceptor properties, potential high conductivity along the  $\pi$ – $\pi$  stacking axis, and advantages such as robustness, thermal stability, and affordability.<sup>69</sup> In the PDI acceptor design, the strategy of introducing large steric groups into the molecule is relatively common, and chemical modifications are usually performed at the imide, *ortho* and *bay* sites in PDI,<sup>70</sup> as shown in Fig. 10.

As early as 1999, Dittmer *et al.*<sup>71</sup> prepared small molecule acceptor PPEI based on PDI through phenylethylation of the imine nitrogen. However, the external quantum conversion efficiency (EQE) of photovoltaic devices based on MEH-PPV: PPEI was only 0.17%. Although the device performance was low, it also indicates the possibility of the PDI structure as an acceptor material.

In order to improve the device efficiency and prevent excessive aggregation between acceptor molecules, the chemical modification of aromatic rings has received increasingly more attention from researchers. In 2006, Shin *et al.*<sup>72</sup> further synthesized two acceptor molecules, 5-PDI and PDI-CN, by modifying the *ortho* position of the PDI aromatic ring on the basis of *N*-cyclohexyl substituted PDI molecules, but the device PCE still did not reach 0.1%. In 2009, Mikroyannidis *et al.*<sup>73</sup> introduced a higher steric hindrance *p*-*tert*-butylphenoxy group at the *ortho* position of the PDI aromatic ring, and changed the

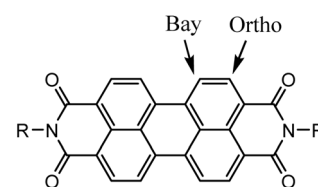


Fig. 10 Common modification sites of the PDI structure.



substituent on the imine nitrogen to a 9-phenanthrene group with a higher steric hindrance. The acceptor molecule PDI-PTBPO was synthesized, and the PCE of the photovoltaic devices based on this acceptor material reached 0.72%. Hartnett *et al.*<sup>74</sup> introduced flexible side chains at the *ortho* position of the aromatic ring and synthesized three small molecule acceptors: Hexyl-PDI, Phenethyl-PDI and Phenyl-PDI. With the increase of the side chain rigidity, the planarity of the acceptor molecules gradually decreased, which resulted in enhanced inter-plane slip of molecules. Devices based on Phenyl-PDI showed the best PV performance ( $V_{OC} = 1.024$  V,  $J_{SC} = 6.56$  mA cm<sup>-2</sup>, FF = 54.59%, PCE = 3.67%). Cai *et al.*<sup>75</sup> synthesized TP-PDI acceptors with four phenyl substitutions at the bay site of the aromatic ring, and PCE of photovoltaic devices prepared by blending with PTB7-Th reached 4.1%.

Similarly, for small PDI-based molecules, multiple acceptor molecules can be connected by a central unit or single bond to prevent excessive aggregation between molecules. Rajaram *et al.*<sup>76</sup> synthesized a PDI dimer Per 1 by directly connecting the imide nitrogen atoms of two PDI molecules through a single bond. Compared with the monomer PDI, the photocurrent density of Per 1 increased significantly, reaching 9.5 mA cm<sup>-2</sup>, and that of PCE reached 2.78%. The same design strategy was used for the small molecule acceptor Bis-PDI-T-EG reported by Zhang *et al.*<sup>77</sup> Bis-PDI-T-EG connects the bay sites of two PDI monomers through a thiophene unit. In order to enhance the intramolecular interaction and intermolecular stacking, an oxygen-containing side chain is introduced to each of the two PDI molecules. The 1 : 1 (wt%) AFM images of the Bis-PDI-T-EG and PBDTTT-CT mixed membranes showed very small aggregation domains, with an average diameter of about 12 nm, indicating that this design strategy effectively reduced the excessive aggregation between the acceptor molecules. Finally, the PBDTTT-CT:Bis-PDI-T-EG photovoltaic devices achieved a PCE of 4.03%. Since then, based on this design strategy, many small molecule acceptors of PDI have appeared, including dimers,<sup>78–82</sup> trimers<sup>83–85</sup> and tetramers,<sup>86–92</sup> and the PCE of photovoltaic devices based on such small molecule acceptors of

oligomeric PDI has reached a maximum of more than 9% (Fig. 11).<sup>93</sup>

## 4 A-D-A and A-DAD-A acceptor materials

### 4.1 A-D-A type acceptor material

In 2013, Winzenberg *et al.*<sup>94</sup> reported on FEHIDT, one of the first A-D-A NFAs, in which the “A” and “D” units are inden-1, 3-dione and fluorene, respectively, and thiophene is used as spacer. The acceptor molecule has a large band gap similar to PDI. It has strong absorption in the range of 400–600 nm. In later works, many researchers modified and adjusted the acceptor molecule, but the PCE was not high.

A major breakthrough in the design of the A-D-A acceptor was the introduction of the indenodithiophene (IDT) building block as the central “D” unit. The first example is an NFA named DC-IDT2T that was reported by Bai *et al.*,<sup>95</sup> where the “A” unit is 1,1-dicyanomethyl-3-indenone (DCI). The results show that the material has a small band gap and strong absorption capacity, extending to the near infrared region. The overall device performance of PBDTTT-T-C, a low band gap donor polymer, was 3.93%.

By modifying DC-IDT2T, two landmark A-D-A acceptors were soon reported. The first one is the IEIC mentioned earlier, which is obtained by adding a 2-ethylhexyl alkyl chain to each spacer thiophene.<sup>57</sup> Then in 2015, Lin<sup>96</sup> reported on the second landmark, an ITIC with a typical A-D-A structure that turned the field of organic photovoltaics into a new light. As the most promising acceptor of its time, ITIC and its derivatives have a unique and important molecular structure, giving it a huge advantage in terms of its photoelectric and photovoltaic properties.<sup>97</sup> From a chemical structure perspective, ITIC and its derivatives consist of two electron-deficient end bases and an electron-rich central nucleus. These units generate powerful push-pull electron effects, making it easy to adjust the photoelectric characteristics, such as the absorption wavelength and

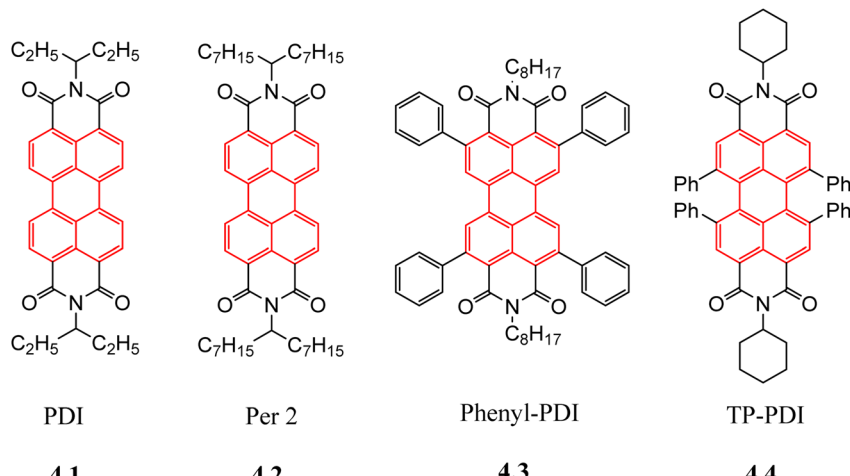


Fig. 11 Molecular structures of SMAs based on PDI.



energy level.<sup>98</sup> In addition, the rigid and planar main chain structure, as well as the strong intermolecular and intramolecular interactions, facilitate charge transfer. At the same time, the side chains connected by ITIC and its derivatives can regulate the solubility of molecules and their compatibility with the donor, resulting in a nice mixture with the desired nanoscale interpenetrating network. The A-D-A molecule has several reactive active sites, which can introduce functional atoms and groups to fine-tune the molecular structure and adjust the molecular properties.

The central thick ring of ITIC is composed of a phenyl ring and two thiophene [3,2-*b*] thiophene molecules, which are bridged by two cyclopentadiene units. Among them, the modification of the electron-rich thick ring core mainly includes replacement of benzene and the thiophene units, an enlarged conjugate backbone length, isomerization, asymmetry, and introduction of heteroatoms. The Zhan group<sup>99</sup> reported on a typical acceptor molecule IDTIC with a benzene-centered pentacyclic indole [1,2-*b*:5,6-*b'*] dithiophene (IDT) as the backbone. When IDTIC is mixed with the polymer donor PDBT-T1,

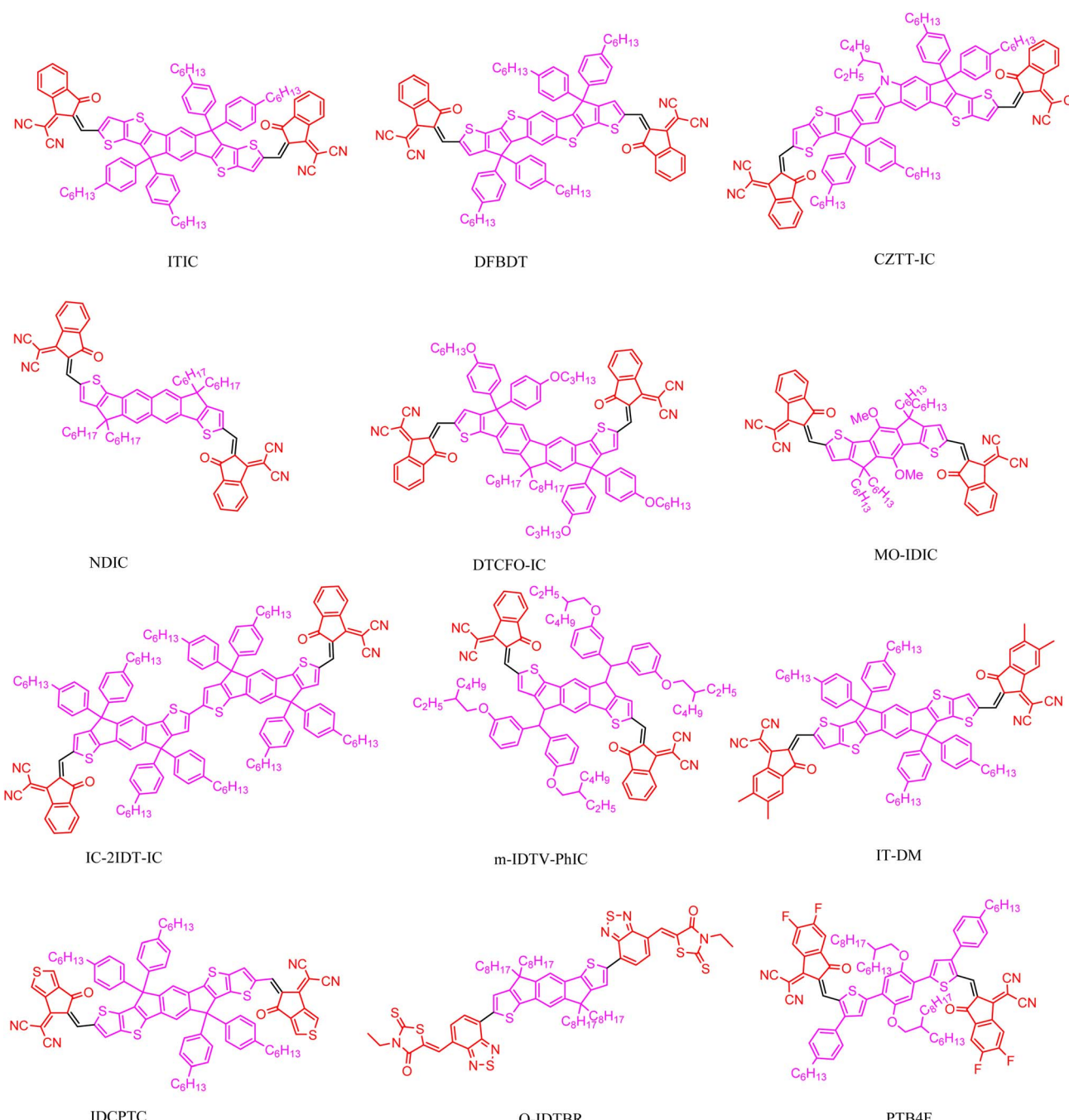


Fig. 12 Molecular structures of A-D-A type acceptors.



the device based on PDBT-T1 IDTIC can achieve 7.39% PCE at a high  $V_{OC}$  of 0.9 V.

At the same time, end groups with strong electron absorption ability play an important role in enhancing the intramolecular and intermolecular interactions and accumulation effects, charge transfer, and photovoltaic performance. 3-(Dicyanomethylene) indigone (IC) and its derivatives are the most commonly used end groups because their electron acceptance is strong enough, and they can be finely controlled by substituting H atoms with halide atoms or alkyls. Li *et al.*<sup>100</sup> designed and synthesized four kinds of ITIC series of acceptor materials, named X-ITIC (X = F, Cl, Br, I), which means a single F, Cl, Br, or I atom is introduced on the original IC end group. Compared to ITIC, the halogenated X-ITIC has a redshifted absorption, deeper energy levels, and stronger crystallinity due to heavy atomic effects and strong electronegativity. With PTPDBDT as the donor, the efficiency of the OSC of X-ITIC is higher (about 9%) than the ITIC counterpart (about 6%) (Fig. 12).

Currently, the ternary strategy has been proven effective in breaking through organic photovoltaics (OPVs). Collaborative improvement of three photovoltaic parameters, especially the third component that is insensitive to proportion, is crucial for efficient three-component systems. Recently, the Sun group<sup>101</sup> introduced a novel asymmetric NFA:BTP-2F2Cl (Fig. 13) based on a PM1:L8-BO mixture to prepare efficient ternary OSCs. Compared to the pure film of L8-BO, the hybrid film of this new molecule exhibits an optimized photoluminescence quantum yield and exciton diffusion length. Through experiments, it was found that the addition of BTP-2F2Cl can adjust the absorption spectrum of the main mixture and increase the HOMO offset of the D/A materials. Researchers also systematically studied the phase separation morphology, finding that the two acceptor materials have good compatibility and can form a stable and uniform mixed phase. With the addition of BTP-2F2Cl, the ternary blend can produce a molecular stacking structure similar to the theme material, but with better performance. It is precisely because of the combined effect of these advantages

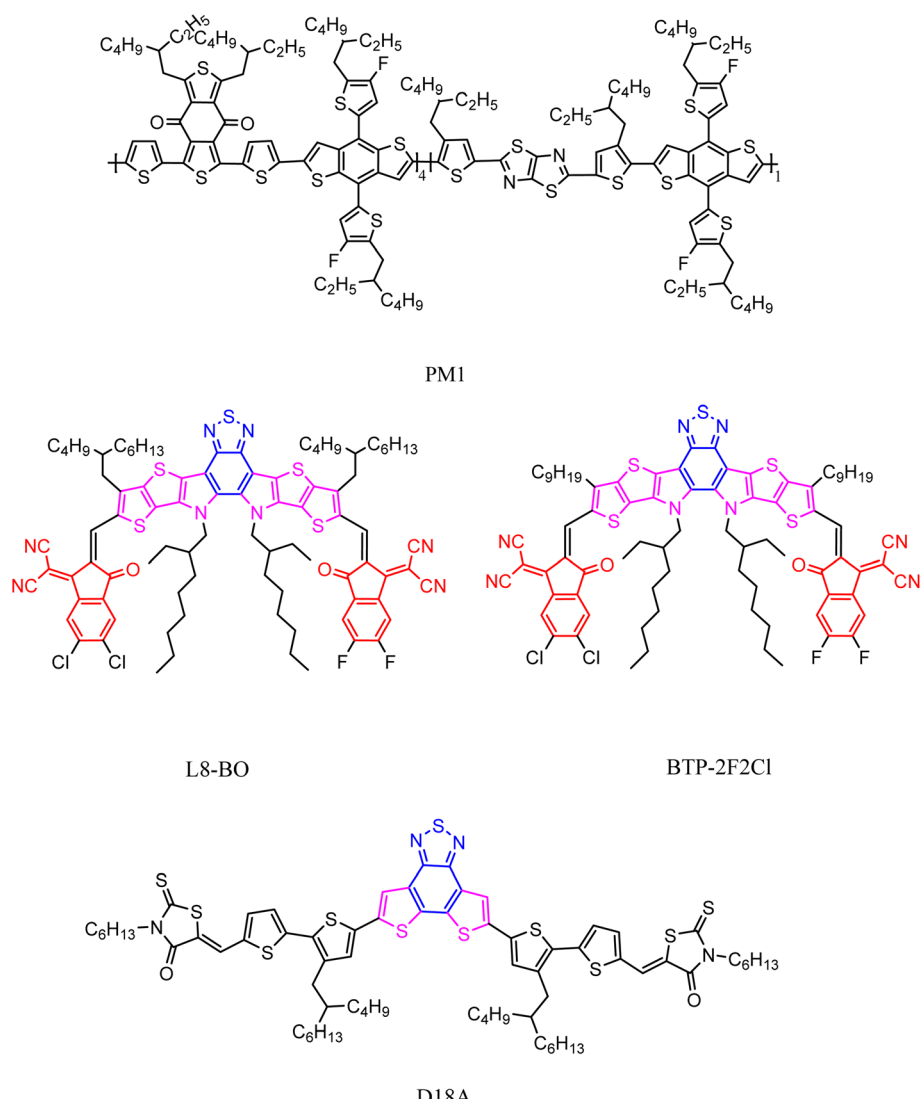


Fig. 13 Molecular structures of PM1, L8-BO and BTP-2F2Cl.



that the non-radiative charge recombination of the ternary system is effectively suppressed, resulting in excellent  $E_{loss}$  performance. Among them, the PCE of the best performing ternary OCS device reached a new high of 19.17%,  $V_{OC}$  of 0.881 V,  $J_{SC}$  of 27.15 mA cm<sup>-2</sup>, and FF of 80.14%. In another study, researchers used polymer PM1 as the donor, small molecule L8-BO as the acceptor, and highly crystalline small molecule D18A as the third component to prepare a series of layered ternary organic photovoltaics. By incorporating 30 wt% D18A into the PM1 layer, the PCE of OPV can be increased from 18.31% to 19.25%, due to the synergistic increase in the short-circuit current density of 27.02 mA cm<sup>-2</sup>, open circuit voltage of 0.909 V, and fill factor of 78.38%.<sup>102</sup>

#### 4.2 A-DA'D-A type acceptor material

The special thick ring structure of the type A-D-A acceptor has a strong and broad absorption, and a tunable molecular

structure related to physicochemical properties. Based on the dominant formation of the type A-D-A acceptor and the structural diversity of the polymer donors, Zou *et al.* designed and proposed a primitive thick ring acceptor BZIC (Y0),<sup>103</sup> showing the conjugated backbone with an A-DA'D-A structure. This design strategy introduces defective electron units into the molecular skeleton of the thick ring molecule, which can improve the luminescence efficiency, while the DA'D unit containing the pyrrole ring has the ability to provide electron and chemical modification sites, which is beneficial to regulating the crystallinity and stacking of molecules. With further modification of the molecular structure and device optimization, the PCE of photovoltaic devices based on the type A-DA'D-A acceptor is already approaching 20%. The rapid development of the A-DA'D-A materials focuses on the thick ring molecular structure, central electron core, end groups and side chains, and the D and A' units on the pyrrole ring.

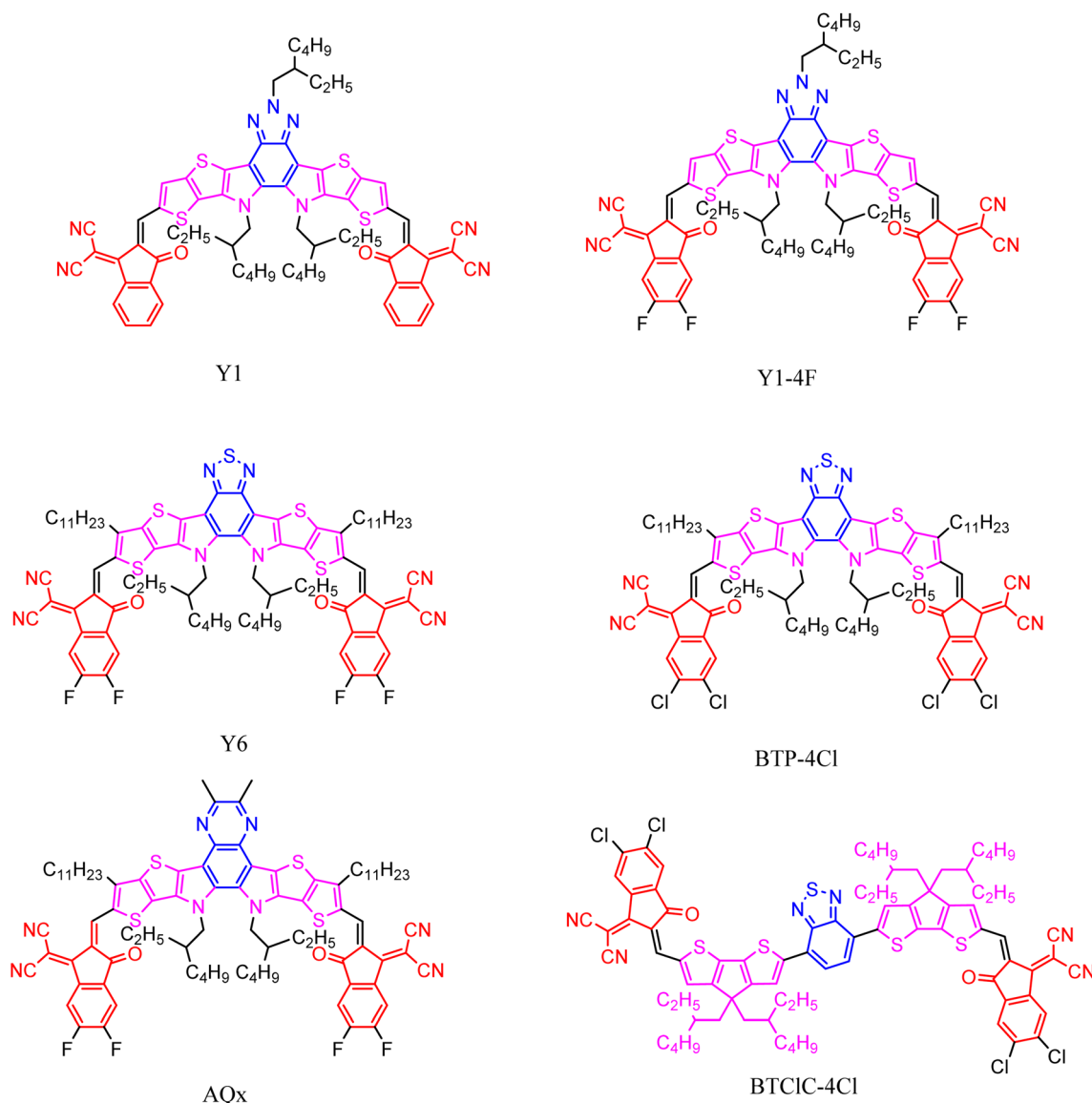


Fig. 14 Molecular structures of A-DA'D-A type acceptors.



With the discovery of Y6 and its derivatives, the study of type A-DA'D-A materials has become an area of increased research focus.<sup>104</sup> Y6 expands the conjugate skeleton based on Y0, introducing alkyl chain modification to replace the acceptor molecule of the electron-deficient central triazole unit, with a photovoltaic performance of over 15% after core and end-group fluorination.<sup>105</sup> In terms of the molecular structure, the good performance of Y6 can be attributed to the following properties. Unlike the electron-donating fused main chain of ITIC, Y6 adopts a donor-acceptor-donor skeleton with a fused ring, fluorinated end groups, and twisted geometric shapes. This enables Y6 to have stronger  $\pi$ - $\pi$  stacking and near-infrared absorption capabilities, thereby enhancing intermolecular stacking, light absorption, and charge transfer performance. Zou and Yuan<sup>106</sup> obtained N3 and N4 with better solubility by adjusting the branching position of 2-ethylhexyl on the nitrogen atom of the Y6 pyrrole ring. With PM6 as the donor material, the PM6:N3 mixture shows the optimal molecular orientation and phase separation size, resulting in the highest device efficiency. Meanwhile, Sun *et al.*<sup>107</sup> introduced branched alkyl chains of different lengths at the thiophene  $\beta$  position of Y6 to improve the molecular packing behavior, yielding 18.32% PCE and 81.5% FF (Fig. 14).

The asymmetric strategy and the introduction of heteroatoms are the most commonly used methods for the study of centrally dense rings. Y6Se and CH1007 (ref. 108 and 109) were synthesized by replacing the sulfur atoms of benzothiadiazole or thiophene [3,2-*b*] thiophene units in Y6 with selenium atoms. The absorption of the two selenium-heterocyclic electron acceptances redshifted to 950 nm, achieving a high  $J_{SC}$  of 28 mA cm<sup>-2</sup> and a PCE of over 17%.

Different end groups have also been used to regulate the optical and electrochemical properties of A-DA'D-A type acceptors.<sup>110,111</sup> Halogenation is a simple and effective method. Yan *et al.*<sup>112</sup> synthesized BTPClBr by changing the positions of chlorine and bromine on the end group. Due to the shallower LUMO energy level, the morphology of the blend is improved, thus enhancing the device performance.<sup>113</sup>

From the perspective of electron acceptor materials, using non-fusion acceptors with strong intramolecular noncovalent interactions is a feasible method to reduce synthesis costs and maintain high efficiency. Furthermore, regulating molecular aggregation, avoiding photosensitive groups, as well as enhancing heat transfer performance can improve the acceptor morphology, photostability, and thermal stability, thereby improving OSC.<sup>114</sup>

In November 2021, Professor Yan He and other researchers<sup>115</sup> collaborated and further studied the influence of side chain configuration on molecular properties by taking m-alkyl phenyl as an externally-substituted side chain BTP-4F derivative. It was proved that the performance of OSCs can be improved by replacing straight chains with branched chains along the external location of NFAs. They designed and synthesized novel NFAs with three different side chains of straight-chain hexyl (BTP-4F-PC6), 2-ethylhexyl (BTP-4F-P2EH) and 3-ethylheptyl (BTP-4F-P3EH) benzene rings. Compared with BTP-4F-PC6, BTP-4F-P2EH and BTP-4F-P3EH exhibit a slight blue shift in the absorption due to

looser intermolecular packing. However, devices based on BTP-4F-P2EH and BTP-4F-P3EH achieve enhanced short-circuit current density ( $J_{SC}$ ) when blended with PBDB-T-2F as the polymer donor. The excessive phase separation of the former two devices is mitigated compared to devices based on BTP-4F-PC6. The results show that BTP-4F-P2EH has good blending form and reduces the non-radiative recombination loss, thus exhibiting the best PCE of 18.22% (BTP-4F-PC6 is 17.22%, BTP-4F-P3EH is 17.57%) and  $V_{OC}$  was 0.880 V. The  $J_{SC}$  was 25.85 mA cm<sup>-2</sup> and the FF was 80.08%.

## 5 Summary and outlook

In summary, this paper focuses on the recent development status of organic solar cell-related materials, including fullerene and its derivatives, polymers, and non-fullerene small molecule acceptor materials. With the continuous improvement of fullerene derivative acceptor materials, the performance of solar cells based on fullerene acceptor materials has been improved to some extent. However, there are still some problems in fullerene materials, such as the low LUMO energy level, narrow absorption spectrum, and small electron mobility. To further improve the fullerene acceptor photovoltaic materials, the following strategies can be adopted:

(1) Introduce metal ions into the fullerene molecules to raise the LUMO level, and the application of transition metal plasma should be expanded, not limited to rare earth metals.

(2) Introducing raw color groups into the fullerene molecules to broaden the absorption spectrum.

For all polymer solar cells, the PCE has been improved from less than 1% based on CN-PPV in early research studies to nearly 10% based on PDI and NDI D-A copolymer acceptors. Recently, devices based on PSMA polymer acceptors have exceeded 15%, reaching the threshold for practical applications. Thus, it is possible all polymer solar cells may outstanding advantages, such as excellent film-forming performance, good bending flexibility, high photostability, and high morphological stability, and are expected to be given priority consideration in the practical application of flexible polymer solar cells.

Finally, for small molecule acceptor materials, the best performance is demonstrated from the thick ring acceptor materials. Adjusting the optical and morphological characteristics of the thick ring acceptors through chemical modification allows the thick ring acceptors to have unique advantages in research. However, to achieve large-scale commercial manufacturing, it is necessary to address green solvent treatment and understand the degradation mechanisms under various environmental conditions to achieve organic photovoltaic devices based on small-molecule acceptor materials that can compete with other solar cell technologies, such as perovskite.

## Data availability

The data that support the findings of this study are available from the corresponding author upon reasonable request.



## Conflicts of interest

There are no conflicts to declare.

## Acknowledgements

This work was financially supported by the National Natural Science Foundation of China (U19A2019) and the Science and Technology Plan Key Project of Hunan Province (2020GK2100).

## References

- 1 S. Huang, C. Qian, X. Liu, *et al.*, A review on flexible solar cells, *Sci. China Mater.*, 2024, **67**(9), 2717–2736.
- 2 D. M. Chapin, C. S. Fuller and G. L. Pearson, A new silicon p–n junction photocell for converting solar radiation into electrical power, *J. Appl. Phys.*, 1954, **25**, 676–677.
- 3 M. Vimala, G. Ramadas, M. Perarasi, *et al.*, A review of different types of solar cell materials employed in bifacial solar photovoltaic panel, *Energies*, 2023, **16**(8), 3605.
- 4 D. Kearns and M. Calvin, Photovoltaic effect and photoconductivity in laminated organic systems, *J. Chem. Phys.*, 1958, **29**(4), 950–951.
- 5 C. W. Tang, Two-layer organic photovoltaic cell, *Appl. Phys. Lett.*, 1986, **48**(2), 183–185.
- 6 N. S. Sarciftci, L. Smilowitz, A. J. Heeger and F. Wudl, Photoinduced electron transfer from a conducting polymer to buckminsterfullerene, *Science*, 1992, **258**, 1474–1476.
- 7 G. Yu and A. J. Heeger, Charge separation and photovoltaic conversion in polymer composites with internal donor/acceptor heterojunctions, *J. Appl. Phys.*, 1995, **78**, 4510–4515.
- 8 A. Kang, W. Zhong, F. Peng, *et al.*, Mastering morphology of non-fullerene acceptors towards long-term stable organic solar cells, *Nat. Commun.*, 2023, **14**, 2688.
- 9 J. C. Hummelen, B. W. Knight, J. Yao, *et al.*, Preparation and characterization of fulleroid and methanofullerene derivatives, *J. Org. Chem.*, 1995, **60**(3), 532–538.
- 10 G. Yu, J. Gao, J. C. Hummelen, *et al.*, Polymer photovoltaic cells: Enhanced efficiencies via a network of internal donor-acceptor heterojunctions, *Science*, 1995, **270**(5243), 1789–1791.
- 11 X. Meng, L. Jiang, C. Wang, *et al.*, Research progress of fullerene acceptor materials in polymeric solar cells, *Sci. Bull.*, 2012, **57**(36), 3437–3449.
- 12 M. M. Wienk, J. M. Kroon, W. J. H. Verhees, *et al.*, Efficient methano[70]fullerene/MDMO-PPV bulk heterojunction photovoltaic cells, *Angew. Chem.*, 2003, **42**(29), 3371–3375.
- 13 F. B. Kooistra, V. D. Mihailescu, L. M. Popescu, *et al.*, New C<sub>84</sub> derivative and its application in a bulk heterojunction solar cell, *Chem. Mater.*, 2006, **18**(13), 3068–3073.
- 14 R. Ganesamoorthy, G. Sathiyan and P. Sakyhivel, Review: Fullerene based acceptors for efficient bulk heterojunction organic solar cell applications, *Sol. Energy Mater. Sol. Cells*, 2017, **161**, 102–148.
- 15 F. B. Kooistra, J. Knol, F. Kastenberg, *et al.*, Increasing the open circuit voltage of bulk-heterojunction solar cells by raising the LUMO level of the acceptor, *Org. Lett.*, 2007, **9**(4), 551–554.
- 16 Y. Zhang, O. Acton, F. Huang, *et al.*, A simple and effective way of achieving highly efficient and thermally stable bulk-heterojunction polymer solar cells using amorphous fullerene derivatives as electron acceptor, *Chem. Mater.*, 2009, **21**(13), 2598–2600.
- 17 H. C. Jung, K. I. Son, T. Kim, *et al.*, Thienyl-substituted methanofullerene derivatives for organic photovoltaic cells, *J. Mater. Chem.*, 2010, **20**, 475–482.
- 18 S.-C. Chuang, C.-W. Chiu, S.-C. Chien, *et al.*, 1-(3-Methoxycarbonyl)propyl-2-selenyl-[6,6]-methanofullerene as a n-type material for organic solar cells, *Synth. Met.*, 2011, **161**(13–14), 1264–1269.
- 19 H. U. Kim, J. H. Kim, H. Kang, *et al.*, Naphthalene-, anthracene-, and pyrene-substituted fullerene derivatives as electron acceptors in polymer-based solar cells, *ACS Appl. Mater. Interfaces*, 2014, **6**(23), 20776–20785.
- 20 G. Zhao, Y. He, Z. Xu, *et al.*, Effect of carbon chain length in the substituent of PCBM-like molecules on their photovoltaic properties, *Adv. Funct. Mater.*, 2010, **20**(9), 1480–1487.
- 21 L. Zheng, Q. Zhou, X. Deng, *et al.*, Methanofullerenes used as electron acceptors in polymer photovoltaic devices, *J. Phys. Chem. B*, 2004, **108**(32), 11921–11926.
- 22 C. Liu, Y. Li, C. Li, *et al.*, New methanofullerenescontaining amide as electron acceptor for construction photovoltaic devices, *J. Phys. Chem. C*, 2009, **113**(52), 21970–21975.
- 23 J. A. Mikroyannidis, A. N. Kabanakis, S. S. Sharma, *et al.*, A simple and effective modification of PCBM for use as an electron acceptor in efficient bulk heterojunction solar cells, *Adv. Funct. Mater.*, 2011, **21**(4), 746–755.
- 24 A. Cabrera-Espinoza, J. G. Sánchez, W. Li, *et al.*, Reducing interfacial recombination in inverted perovskite solar cells with selenophene-substituted PCBM: Comparison with thiophene and furan substitution, *ChemSusChem*, 2024, e202400901.
- 25 R. B. Ross, C. M. Cardona, D. M. Guldin, *et al.*, Endohedral fullerenes for organic photovoltaic devices, *Nat. Mater.*, 2009, **8**(3), 208–212.
- 26 M. Lenes, F. B. Kooistra, S. C. Veenstra, *et al.*, Fullerene bisadducts for enhanced open-circuit voltages and efficiencies in polymer solar cells, *Adv. Mater.*, 2008, **20**(11), 2116–2119.
- 27 M. Lenes, S. W. Shelton, A. B. Sieval, *et al.*, Electron trapping in higher adduct fullerene-based solar cells, *Adv. Funct. Mater.*, 2009, **19**(18), 3002–3007.
- 28 Y. He, B. Peng, Z. Guangjin, *et al.*, Indene addition of [6,6]-phenyl-C<sub>61</sub>-butyric acid methyl ester for high-performance acceptor in polymer solar cells, *J. Phys. Chem. C*, 2011, **115**(10), 4340–4344.
- 29 S. A. Backer, K. Sivula, D. F. Kavulak, *et al.*, High efficiency organic photovoltaics incorporating a new family of soluble fullerene derivatives, *Chem. Mater.*, 2007, **19**(12), 2927–2929.



30 K. Matsumoto, K. Hashimoto, M. Kamo, *et al.*, Design of fulleropyrrolidine derivatives as an acceptor molecule in a thin layer organic solar cell, *J. Mater. Chem.*, 2010, **20**, 9226–9230.

31 Y. Matsuo, A. Iwashita, Y. Abe, *et al.*, Regioselective synthesis of 1,4-di(organo)[60]fullerenes through DMF-assisted monoaddition of silylmethylgrignard reagents and subsequent alkylation reaction, *J. Am. Chem. Soc.*, 2008, **130**(46), 15429–15436.

32 Y. Matsuo, Y. Sato, T. Niinomi, *et al.*, Columnar structure in bulk heterojunction in solution-processable three-layered p-i-n organic photovoltaic devices using tetrabenzoporphyrin precursor and silylmethyl[60]fullerene, *J. Am. Chem. Soc.*, 2009, **131**(44), 16048–16050.

33 Y. He, H.-Y. Chen, J. Hou, *et al.*, Indene-C(60) bisadduct: a new acceptor for high-performance polymer solar cells, *J. Am. Chem. Soc.*, 2010, **132**(4), 1377–1382.

34 X. Meng, W. Zhang, Z. Tan, *et al.*, Dihydronaphthyl-based [60]fullerene bisadducts for efficient and stable polymer solar cells, *Chem. Commun.*, 2012, **48**(3), 425–427.

35 J.-S. Nam, Y. Seo, J. Han, *et al.*, Exploring endohedral metallofullerenes for advanced thin-film device applications toward next-generation electronics, *Chem. Mater.*, 2023, **35**(20), 8323–8337.

36 L. Feng, S. Wang, H. Huang, *et al.*, Dynamic metastable characteristics of carbon cages embedded with Er<sub>2</sub>C<sub>2</sub>, *Inorg. Chem.*, 2023, **62**(35), 14216–14227.

37 Z. Zhang and Y. Li, Polymerized small-molecule acceptors for high-performance all-polymer solar cells, *Angew. Chem., Int. Ed.*, 2020, **133**(9), 4470–4481.

38 Y. Zou, J. Hou, C. Yang, *et al.*, A novel n-type conjugated polymer DOCN-PPV: Synthesis, optical, and electrochemical properties, *Macromolecules*, 2006, **39**(26), 8889–8891.

39 G. Sang, Y. Zou, Y. Huang, *et al.*, All-polymer solar cells based on a blend of poly[3-(10-n-octyl-3-phenoxythiazine-vinylene)thiophene-co-2,5-thiophene] and poly[1,4-dioctyloxy-p-2,5-dicyanophenylenevinylene], *Appl. Phys. Lett.*, 2009, **94**(19), 193302.

40 W. Khelifi and C.-K. Luscombe, Recent developments in indacenodithiophene and indacenodithienothiophene-based donor-acceptor conjugated polymers: From design to device performance in organic electronics, *Prog. Polym. Sci.*, 2024, **151**, 101804.

41 X. Zhan, Z. Tan, B. Domercq, *et al.*, A high-mobility electron-transport polymer with broad absorption and its use in field-effect transistors and all-polymer solar cells, *J. Am. Chem. Soc.*, 2007, **129**(23), 7246–7247.

42 Y. Zhang, Q. Wan, X. Guo, *et al.*, Synthesis and photovoltaic properties of an n-type two-dimension-conjugated polymer based on perylene diimide and benzodithiophene with thiophene conjugated side chains, *J. Mater. Chem. A*, 2015, **3**(36), 18442–18449.

43 X. Guo and M. D. Watson, Conjugated polymers from naphthalene bisimide, *Org. Lett.*, 2008, **10**(23), 5333–5336.

44 N. Zheng, K. Mahmood, W. Zhong, *et al.*, Improving the efficiency and stability of non-fullerene polymer solar cells by using N2200 as the Additive, *Nano Energy*, 2019, **58**, 724–731.

45 Z. Zhang, Y. Yang, J. Yao, *et al.*, Constructing a strongly absorbing low-bandgap polymer acceptor for high-performance all-polymer solar cells, *Angew. Chem., Int. Ed.*, 2017, **56**(43), 13503–13507.

46 H. Yao, F. Bai, H. Hu, *et al.*, Efficient all-polymer solar cells based on a new polymer acceptor achieving 10.3% power conversion efficiency, *ACS Energy Lett.*, 2019, **4**(2), 417–422.

47 Y. Li, Z. Jia, Q. Zhang, *et al.*, Toward efficient all-polymer solar cells via halogenation on polymer acceptors, *ACS Appl. Mater. Interfaces*, 2020, **12**(29), 33028–33038.

48 Q. Fan, W. Su, S. Chen, *et al.*, Mechanically robust all-polymer solar cells from narrow band gap acceptors with hetero-bridging atoms, *Joule*, 2020, **4**(3), 658–672.

49 Q. Fan, R. Ma, T. Liu, *et al.*, 10.13% efficiency all-polymer solar cells enabled by improving the optical absorption of polymer acceptors, *Sol. RRL*, 2020, **4**(6), 2000142.

50 Q. Fan, W. Su, S. Chen, *et al.*, A non-conjugated polymer acceptor for efficient and thermally stable all-polymer solar cells, *Angew. Chem., Int. Ed.*, 2020, **59**(45), 19835–19840.

51 T. Jia, J. Zhang, W. Zhong, *et al.*, 14.4% efficiency all-polymer solar cell with broad absorption and low energy loss enabled by a novel polymer acceptor, *Nano Energy*, 2020, **72**, 104718.

52 P. Bi, T. Zhang, Y. Cui, *et al.*, High-performance binary all-polymer solar cells with efficiency over 18.3% enabled by tuning phase transition kinetics, *Adv. Energy Mater.*, 2023, **13**(40), 2302252.

53 F.-G. Guijarro, P. De la cruz, K. Khandelwal, *et al.*, Effects of halogenation on cyclopentadithiophenevinylene-based acceptors with excellent responses in binary organic solar cells, *ACS Appl. Mater. Interfaces*, 2023, **15**(17), 21296–21305.

54 H. Wang, C. Cao, H. Chen, *et al.*, Oligomeric acceptor: A “two-in-one” strategy to bridge small molecules and polymers for stable solar devices, *Angew. Chem., Int. Ed.*, 2022, **61**(23), e202201844.

55 L. Zhang, Z. Zhang, D. Deng, *et al.*, “N-π-N” type oligomeric acceptor achieves an OPV efficiency of 18.19% with low energy loss and excellent stability, *Advanced Science*, 2022, **9**(23), 2202513.

56 Y. Fu, F. Wang, X. Fang, *et al.*, Progress in electron acceptor materials for non-fullerene small-molecule organic solar cells, *J. Chem.*, 2014, **72**(02), 158–170.

57 Y. Lin, Z. Zhang, H. Bai, *et al.*, High-performance fullerene-free polymer solar cells with 6.31% efficiency, *Energy Environ. Sci.*, 2015, **8**(2), 610–616.

58 L. Hong, H. Yao, R. Yu, *et al.*, Investigating the trade-off between device performance and energy loss in nonfullerene organic solar cells, *ACS Appl. Mater. Interfaces*, 2019, **11**(32), 29124–29131.

59 L. Ma, S. Zhang, J. Zhu, *et al.*, Completely non-fused electron acceptor with 3D-interpenetrated crystalline structure enables efficient and stable organic solar cell, *Nat. Commun.*, 2021, **12**, 5039.



60 X. Wang, H. Lu, Y. Liu, *et al.*, Simple nonfusing electron acceptors with 3D network packing structure boosting the efficiency of organic solar cells to 15.44%, *Adv. Energy Mater.*, 2021, **11**(15), 2102591.

61 D. Ma, Q. Zhang and C. Li, Unsymmetrically chlorinated non-fused electron acceptor leads to high-efficiency and stable organic solar cells, *Angew. Chem., Int. Ed.*, 2022, **62**(5), e202214931.

62 J. E. Anthony, A. Facchetti, M. Heeney, *et al.*, n-Type organic semiconductors in organic electronics, *Adv. Mater.*, 2010, **22**(34), 3876–3892.

63 A. P. H. J. Schenning, J. v. Herrikhuyzen, P. Jonkheijm, *et al.*, Photoinduced electron transfer in hydrogen-bonded oligo(p-phenylene vinylene)-perylene bisimide chiral assemblies, *J. Am. Chem. Soc.*, 2002, **124**(35), 10252–10253.

64 E. Ahmed, G. Ren, F. S. Kim, *et al.*, Design of new electron acceptor materials for organic photovoltaics: Synthesis, electron transport, photophysics, and photovoltaic properties of oligothiophene-functionalized naphthalene diimides, *Chem. Mater.*, 2011, **23**(20), 4563–4577.

65 R. Fonando, Z. Mao, *et al.*, Tuning the organic solar cell performance of acceptor 2,6-dialkylaminonaphthalene diimides by varying a linker between the Imide nitrogen and a thiophene group, *J. Phys. Chem. C*, 2014, **118**(7), 3433–3442.

66 W. Xue, J. Huang, Z. Niu, *et al.*, Dimeric naphthalene diimide based small molecule acceptors: synthesis, characterization, and photovoltaic properties, *Tetrahedron*, 2014, **70**(32), 4726–4731.

67 A. Gupta, R. V. Hangarge, X. Wang, *et al.*, Crowning of dibenzosilole with a naphthalene diimide functional group to prepare an electron acceptor for organic solar cells, *Dyes Pigm.*, 2015, **120**(1), 314–321.

68 Y. Liu, L. Zhang, H. Lee, *et al.*, NDI-based small molecule as promising nonfullerene acceptor for solution-processed organic photovoltaics, *Adv. Energy Mater.*, 2015, **5**(12), 1500195.

69 S. Mitra, R. Sudipta, G. Narendra-Nath, *et al.*, Designed and synthesized ANTPABA-PDI nanomaterial as an acceptor in inverted solar cell at ambient atmosphere, *Nanotechnology*, 2023, **34**(31), 315704.

70 V. Sharma, J. D. B. Koenig, G. C. Welch, *et al.*, Perylene diimide based nonfullerene acceptors: Top performers and an emerging class featuring N-annulation, *J. Mater. Chem. A*, 2021, **9**(11), 6775–6789.

71 J. J. Dittmer, K. Petritsch, E. A. Marseglia, *et al.*, Photovoltaic properties of MEH-PPV/PPEI blend devices, *Synth. Met.*, 1999, **102**(1–3), 879–880.

72 W. s. Shin, H. H. Jeong, M. K. Kim, *et al.*, Effects of functional groups at perylene diimide derivatives on organic photovoltaic device application, *J. Mater. Chem.*, 2006, **16**(4), 384–390.

73 J. A. Mikroyannidis, M. M. Stylianakis, P. Suresh, *et al.*, Efficient hybrid bulk heterojunction solar cells based on phenylenevinylene copolymer, perylene bisimide and TiO<sub>2</sub>, *Sol. Energy Mater. Sol. Cells*, 2009, **93**(10), 1792–1800.

74 P. E. Hartnett, A. Timalsina, H. S. S. Ramakrishna Matte, *et al.*, Slip-stacked perylenediimides as an alternative strategy for high efficiency nonfullerene acceptors in organic photovoltaics, *J. Am. Chem. Soc.*, 2014, **136**(46), 16345–16356.

75 Y. Cai, L. Huo, X. Sun, *et al.*, High performance organic solar cells based on a twisted bay-substituted tetraphenyl functionalized perylene diimide electron acceptor, *Adv. Energy Mater.*, 2015, **5**(11), 1500032.

76 S. Rajaram, R. Shivanna, S. Kumar, *et al.*, Nonplanar perylene diimides as potential alternatives to fullerenes in organic solar cells, *Phys. Chem. Lett.*, 2012, **3**(17), 2405–2408.

77 X. Zhang, Z. Lu, L. Ye, *et al.*, A potential perylene diimidedimer-based acceptor material for highly efficient solution-processed nonfullerene organic solar cells with 4.03% efficiency, *Adv. Mater.*, 2013, **25**(40), 5791–5797.

78 W. Jiang, L. Ye, X. Li, *et al.*, Bay-linked perylene bisimides as promising nonfullerene acceptors for organic solar cells, *Chem. Commun.*, 2014, **50**(8), 1024–1026.

79 M. Dong, D. Sun, C. Zhong, *et al.*, High-performance solution-processed nonfullerene organic solar cells based on selenophene-containing perylene bisimide acceptor, *J. Am. Chem. Soc.*, 2016, **138**(1), 375–380.

80 Q. Yan, Y. Zhou, Y. Zheng, *et al.*, Towards rational design of organic electron acceptors for photovoltaics: A study based on perylenediimide derivatives, *Chem. Sci.*, 2013, **4**(12), 4389–4394.

81 J. Liu, S. Chen, D. Qian, *et al.*, Fast charge separation in a nonfullerene organic solar cell with a small driving force, *Nat. Energy*, 2016, **1**(7), 16089.

82 Y. Lin, J. Wang, S. Dai, *et al.*, A twisted dimeric perylene diimideelectron acceptor for efficient organic solar cells, *Adv. Energy Mater.*, 2014, **4**(13), 1400420.

83 P. Su, G. Ran, H. Wang, *et al.*, Intramolecular and intermolecular interaction switching in the aggregates of perylene diimide trimer: Effect of hydrophobicity, *Molecules*, 2023, **28**(7), 3003.

84 N. Liang, K. Sun, Z. Zhong, H. Yao, *et al.*, Perylene diimidetrimer-based bulk heterojunction organic solar cells with efficiency over 7%, *Adv. Energy Mater.*, 2016, **6**(11), 1600060.

85 Y. Duan, X. Xu, H. Yan, *et al.*, Pronounced effects of a triazine core on photovoltaic performance-efficient organic solar cells enabled by a PDI trimer-based small molecular acceptor, *Adv. Mater.*, 2017, **29**(7), 1605115.

86 Y. Liu, *et al.*, A tetraphenylethylene core-based 3D structure small molecular acceptor enabling efficient nonfullerene organic solar cells, *Adv. Mater.*, 2015, **27**(6), 1015–1020.

87 S. Liu, C. Wu, C. Li, *et al.*, A tetraperylene diimides based 3D nonfullereneacceptor for efficient organic photovoltaics, *Adv. Sci.*, 2015, **2**(4), 1500014.

88 Y. Liu, J. Y. L. Lai, S. Chen, *et al.*, Efficient nonfullerene polymer solar cells enabled by tetrahedron-shaped core based 3D-structure small-molecular electron acceptors, *J. Mater. Chem. A*, 2015, **3**(26), 13632–13636.



89 H. Lin, S. Chen, H. Hu, *et al.*, Reduced intramolecular twisting improves the performance of 3D molecular acceptors in non-fullerene organic solar cells, *Adv. Mater.*, 2016, **28**(38), 8546–8551.

90 J. Lee, R. Singh, H. S. Dong, *et al.*, A nonfullerene small molecule acceptor with 3D interlocking geometry enabling efficient organic solar cells, *Adv. Mater.*, 2016, **28**(1), 69–76.

91 A. Zhang, L. Cheng, F. Yang, *et al.*, An electron acceptor with porphyrin and perylene bisimides for efficient non-fullerene solar cells, *Angew. Chem., Int. Ed.*, 2017, **56**(10), 2694–2698.

92 Y. Han, L. Arungiri, L. Zhang, *et al.*, Transannularly conjugated tetrameric perylene diimide acceptors containing [2.2]paracyclophane for non-fullerene organic solar cells, *J. Mater. Chem. A*, 2020, **8**(14), 6501–6509.

93 G. Zhang, J. Zhao, P. C. Y. Chow, *et al.*, Nonfullerene acceptor molecules for bulk heterojunction organic solar cells, *Chem. Rev.*, 2018, **118**(7), 3447–3507.

94 K. N. Winzenberg, P. Kemppinen, F. H. Scholes, *et al.*, Indan-1,3-dione electron-acceptor small molecules for solution-processable solar cells: a structure–property correlation, *Chem. Commun.*, 2013, **49**(56), 6307–6309.

95 H. Bai, Y. Wang, C. Pei, *et al.*, An electron acceptor based on indacenodithiophene and 1,1-dicyanomethylene-3-indanone for fullerene-free organic solar cells, *J. Mater. Chem. A*, 2014, **3**(5), 1910–1914.

96 Y. Lin, J. Wang, Z. Zhang, *et al.*, An electron acceptor challenging fullerenes for efficient polymer solar cells, *Adv. Mater.*, 2015, **27**(7), 1170–1174.

97 T.-Y. Huang, A.-P. L. brun, B. Sochor, *et al.*, Nanometer-thick ITIC bulk heterojunction films as non-fullerene acceptors in organic solar cells, *ACS Appl. Nano Mater.*, 2024, **7**(15), 17588–17595.

98 J. Zhu, L. Lv, T. Dai, *et al.*, Side-chain engineering in ITIC skeleton enabling as-cast organic solar cells with reduced energy loss and improved vertical phase distribution, *ACS Mater. Lett.*, 2024, **6**(6), 2100–2110.

99 Y. Lin, T. Li, F. Zhao, *et al.*, Structure evolution of oligomer fused-ring electron acceptors toward high efficiency of As-cast polymer solar cells, *Adv. Energy Mater.*, 2016, **6**(18), 1600845.

100 F. Yang, C. Li, W. Lai, *et al.*, Halogenated conjugated molecules for ambipolar field-effect transistors and non-fullerene organic solar cells, *Mater. Chem. Front.*, 2017, **1**(7), 1389–1395.

101 R. Sun, Y. Wu, X. Yang, *et al.*, Single-junction organic solar cells with 19.17% efficiency enabled by introducing one asymmetric guest acceptor, *Adv. Mater.*, 2022, **34**(26), 2110147.

102 H. Tian, Y. Ni, W. Zhang, *et al.*, Over 19.2% efficiency of layer-by-layer organic photovoltaics enabled by a highly crystalline material as an energy donor and nucleating agent, *Energy Environ. Sci.*, 2024, **17**, 5173–5182.

103 L. Feng, J. Yuan, Z. Zhang, *et al.*, Thieno[3,2-b]pyrrolo-fused pentacyclic benzotriazole-based acceptor for efficient organic photovoltaics, *Appl. Mater. Interfaces*, 2017, **9**(37), 31985–31992.

104 Y. Xiang, C. Xu and S. Zheng, Increasing charge carrier mobility through modifications of terminal groups of Y6: A theoretical study, *Int. J. Mol. Sci.*, 2023, **24**(10), 8610.

105 J. Yuan, Y. Zhang, L. Zhou, *et al.*, Single-junction organic solar cell with over 15% efficiency using fused-ring acceptor with electron-deficient core, *Joule*, 2019, **3**(4), 1–12.

106 K. Jiang, Q. Wei, J. Y. L. Lai, *et al.*, Alkyl chain tuning of small molecule acceptors for efficient organic solar cells, *Joule*, 2019, **3**(12), 3020–3033.

107 C. Li, J. Zhou, J. Song, *et al.*, Non-fullerene acceptors with branched side chains and improved molecular packing to exceed 18% efficiency in organic solar cells, *Nat. Energy*, 2021, **6**, 605–613.

108 Z. Zhang, Y. Li, G. Cai, *et al.*, Selenium heterocyclic electron acceptor with small urbachenergy for As-cast high-performance organic solar cells, *J. Am. Chem. Soc.*, 2020, **142**(44), 18741–18745.

109 F. Lin, K. Jiang, K. Werner, *et al.*, A non-fullerene acceptor with enhanced intermolecular  $\pi$ -core interaction for high-performance organic solar cells, *J. Am. Chem. Soc.*, 2020, **142**(36), 15246–15251.

110 Z. Wang, M. Ji, A. Tang, *et al.*, Shamrock-shaped non-fullerene acceptors enable high-efficiency and high-voltage organic photovoltaics, *Energy Environ. Sci.*, 2024, **17**(11), 3868–3877.

111 C. L. Wen, J. Yuan, Z. Zhang, *et al.*, Aromatic side chain manipulation in A-DA'D-A type acceptors for organic photovoltaics, *Mater. Chem. Front.*, 2024, **8**(21), 3587–3595.

112 Z. Luo, R. Ma, Z. Chen, *et al.*, Altering the positions of chlorine and bromine substitution on the end group enables high-performance acceptor and efficient organic solar cells, *Adv. Energy Mater.*, 2020, **10**(44), 2002649.

113 W. Wei, X. Yuan, J. Zhong, *et al.*, High-efficiency organic solar cells from low-cost pentacyclic fused-ring electron acceptors via crystal engineering, *Energy Environ. Sci.*, 2024, **17**(18), 6627–6639.

114 W. Qinya, J. Yuan, Y. Yi, *et al.*, Y6 and its derivatives: Molecular design and physical mechanism, *Natl. Sci. Rev.*, 2021, **8**(8), nwab121.

115 J. Zhang, F. Bai, X. Xu, *et al.*, Alkyl-chain branching of non-fullerene acceptors flanking conjugated side groups toward highly efficient organic solar cells, *Adv. Energy Mater.*, 2021, **11**(47), 2102596.

